Density Matrix Renormalization Group Analysis of Spin Chains and Quantum Hall Systems

Emil Johansson Bergholtz

Master's Thesis

Department of Physics
Stockholm University

13th December 2002

Abstract

There is often a need for simplification and approximations in condensed matter physics. A very powerful method for these purposes, the Density Matrix Renormalization Group, is studied in this thesis. The DMRG method has had tremendous success when it has been applied to one-dimensional systems such as the antiferromagnetic Heisenberg spin chain, the Ising model and the XY-model. In this thesis, various previously known properties of the antiferromagnetic Heisenberg chain are presented as well as a new application to a Quantum Hall system. The QH system that is examined consists of a two-dimensional electron gas on a cylinder with a strong magnetic field perpendicular to the electron layer. For a thin cylinder, a homogenous ground state is found at filling factor $\nu = \frac{1}{2}$ and examined in some detail. Furthermore, we observe particle as well as hole excitations in the $\nu = \frac{1}{2} \pm \varepsilon$ ground states. There is reason to believe that relatively small adjustments would make it possible to study the fractionally charged Quantum Hall states corresponding to filling factors $\nu = \frac{1}{2m+1}$.

Acknowledgements

First of all I would like to thank my supervisor Anders Karlhede for introducing me to this subject and for being very helpful during all stages of my work on this thesis. During this work on I have learned a lot of physics, programming and how to deal with a large project. It has also opened a new and interesting field of physics that I knew almost nothing about prior to this work.

I would also like to thank my brother Olle for helping me with all kinds of graphics related problems and all the people in the Field and Particle Theory group that has been helping me in various ways.

Contents

Chapter 1

Introduction and Outline

Strongly correlated systems are among the most active areas of theoretical condensed matter physics today. The models describe systems where a large number of particles interact strongly with each other and therefore cannot be analyzed starting from properties of single particles. Even though there exists quantum many body systems that are relatively easy to understand many of them are extremely complicated. This can easily be seen by studying a rather simple many particle system of N free charged particles that interact according to Coulomb's law in vacuum. In this case the Schrödinger equation reads

$$[-\frac{\hbar^2}{2}\sum_{i=1}^{N}\frac{\nabla_i^2}{m_i}+\frac{1}{4\pi\epsilon_0}\sum_{i<j}\frac{q_i q_j}{|\vec{r}_i-\vec{r}_j|}]\Psi(\{\vec{r}_i\},t)=i\hbar\frac{\partial\ \Psi(\{\vec{r}_i\},t)}{\partial t}; \qquad (1.1)$$

which is clearly far to hard to solve, even numerically, for systems of large N. These systems often need a description based on collective phenomena when a huge amount of atoms or particles interact. In order to find such a description one must look for a simplified model or a so called effective theory. When such a theory is constructed it may still be very hard or even impossible to calculate the properties that one is interested in analytically. Thus one must also find good numerical prescriptions to deal with that problem.

There are many different ways to simplify the calculations for strongly correlated systems and one of the most successful ones is a method called Density Matrix Renormalization Group theory (DMRG), invented by White [1] in 1992. The method obeys the variational principle because it does not introduce unphysical states. It only gives a method of finding the most relevant ones. This particular method has had tremendous success over the last decade when it has been applied to one-dimensional systems such as the ferro- and antiferromagnetic Heisenberg spin chains, the Ising model and the XY- model.

Another hot area of theoretical condensed matter physics is the quantum Hall effect. This area deals with interacting electrons moving in two spatial dimensions in a very strong perpendicular magnetic field. This is also an example of a strongly correlated system where there is a need for effective theories and numerical methods.

Several phenomena observed in QH systems, such as the fractional QH effect[1] and Skyrmions[2], are based on collective rather than on single electron properties. Despite this Laughlin [2] was able to give a microscopic understanding of the fractional quantum Hall systems by providing a very good trial wave function for the many particle ground state.

In this thesis we first investigate properties of DMRG for some previously studied systems and then we explore the possibility of applying the successful DMRG methods to a quantum Hall system.

The basic concepts of DMRG are presented in chapter two and these are implemented on the antiferromagnetic Heisenberg chain in chapter three. The latter chapter also deals with the description of the Heisenberg, XY and Ising Hamiltonians and contains some of the results that we have achieved with our DMRG program.

Chapter four deals with a quantum Hall system which consists of a two-dimensional electron gas on a cylinder with a strong magnetic field perpendicular to the electron layer. The Hamiltonian is analyzed and some approximations are made in order to make it possible to apply the DMRG method. These methods are new and we have been able to extract interesting results for the $\nu = 1/2$ ground state on a thin cylinder where we find a homogenous state. The results are presented as well as the strengths and weaknesses of the approach. Conclusions and an outlook are contained in the fifth chapter.

[1] Particle excitations may have fractional charges ($q = e/3, e/5, \ldots$) at low temperatures in the fractional QH effect.

[2] Skyrmions are particles (or topological objects) formed by the collective motion of several electron. They have the same charge as the particle excitations but the spin is higher.

Chapter 2

Density Matrix Renormalization Group

Renormalization is used in many different areas of theoretical physics such as quantum field theory and the theory of critical phenomena. However we will only consider the Density Matrix Renormalization Group [1] and its precursor, the one-dimensional standard numerical Renormalization Group (RG) [3], in this chapter.

The objective of these renormalization methods is to find effective descriptions of large systems. This is done by starting with a small system that is well known and then increase the size gradually. At the same time as much irrelevant information as possible is discarded. This procedure is motivated by the fact that the number of quantum states of a system increases exponentially with the number of particles and therefore the computers of today are only able to treat very small systems by use of exact methods. However there are many examples of macroscopic systems[1] where quantum effects are crucial. In the following we provide a systematic way of dealing with some of these systems.

2.1 The 1-D standard numerical renormalization group

Let us consider a chain that one first breaks into a set of identical blocks A, as shown in figure 2.1. From two neighboring blocks A, the corresponding Hamiltonians H_A and the interactions between the blocks, one forms new and larger blocks AA and Hamiltonians H_{AA}.

Figure 2.1: *A chain divided into identical blocks A.*

[1] Two famous examples are the quantum Hall effect and the Bose-Einstein condensation.

In order to reduce the number of states kept one diagonalizes the Hamiltonian matrix H_{AA} and uses the m lowest lying eigenstates (if one wants to study the ground state) to form a new simpler Hamiltonian $H_{A'}$ which now represents a block twice as large, as in figure 2.2. In doing this, one assumes that only the lowest lying block eigenstates play a dominant role in forming larger blocks at later iterations.

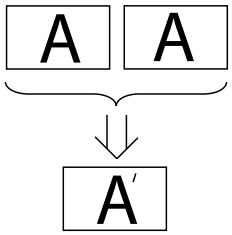

Figure 2.2: *Two identical blocks A that are used to form A'.*

The procedure above represents one iteration and it is repeated until the desired size is reached. In a given iteration one must represent the block AA by m^2 states since each of the blocks A is represented by m states. A slightly more general case is if one connects two neighboring blocks A and B that are represented by m and n states respectively. In this case the block AB is clearly represented by $m \times n$ states.

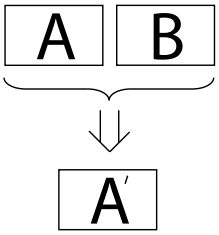

Figure 2.3: *Two blocks A and B that are used to form A'.*

The result for the blocks A and B will be important later since it makes it possible to keep many states m in every iteration as long as the number of states n of the added block B is sufficiently small.

To form the effective Hamiltonian we consider the approach used by Wilson [3], involving a change of basis to the new set of eigenstates. This truncation procedure can be written as

$$H_{A'} = OH_{AB}O^{\dagger} \tag{2.1}$$

where O is an $m \times d$ matrix when d is the dimension of H_{AB} and m is the number of states kept. In the standard numerical renormalization group procedure the rows of O are the m lowest lying eigenstates of H_{AB}.

It is helpful to notice that no unphysical states are introduced during the calculations and therefore a study of the ground state obeys the variational principle which states that

$$E_{variational} \geq E_0, \tag{2.2}$$

where E_0 is the exact ground state energy. Thus the calculated energy gives an upper bound for the ground state energy.

2.2 Optimal states from density matrices

The lowest energy eigenstates of H_{AB} seem to be the natural states to keep but as we shall see they are not optimal simply because they are not taking the interactions with the surrounding blocks into account. An alternative approach, proposed by White and Noack [4], is the superblock method. In this method, one diagonalizes a larger system, the superblock, composed of at least three[2] blocks including the two blocks A and B which are used to form A'.

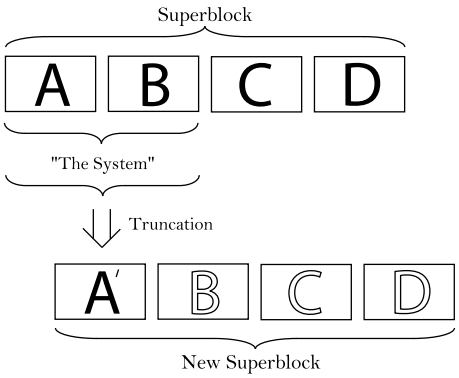

Figure 2.4: *A scheme of how an iteration of the superblock method is carried out.*

The states of the superblock are projected onto AB and these projected[3] states are kept. However, for a many-particle state, the projection can be done in many different ways. This raises the question of which states are the most important ones. The density matrix provides a good answer according to White [1, 5]. As it turns out the eigenstates with the largest eigenvalues of the density matrix[4] for AB, produced from the ground state[5] of the superblock, are the

[2] We use four blocks because it will make it easier, as the reader will see later, to take advantage of certain symmetries.

[3] The projection have the same role as the truncation in the standard RG.

[4] If you are unfamiliar with density matrices you should review Feynman's [7] or Sakurai's [6] introductions to the subject.

[5] Or any other state one wants to study.

optimal states to keep in a certain well defined sense.

Assume that we have diagonalized the superblock and extracted a particular state $|\,\Psi\,\rangle$, usually the ground state. Let $|\,i\,\rangle$, $i = 1, \ldots, n$, be a complete set of states for the system AB and let $|\,j\,\rangle$, $j = 1, \ldots, J$, be the states of the rest of the superblock, i.e. the surroundings. We can then write[6]

$$|\,\Psi\,\rangle = \sum_{ij} \psi_{ij} |\,i\,\rangle |\,j\,\rangle. \tag{2.3}$$

However we do not always want to keep all the states $|\,i\,\rangle$. If the number of states n required to describe $|\,\Psi\,\rangle$ exactly, is greater than the number of states m kept in each iteration we cannot represent $|\,\Psi\,\rangle$ exactly with only m states. Hence we want to construct a set of orthogonal states $|\,u^\alpha\,\rangle = \sum_i u_i^\alpha |\,i\,\rangle$, $\alpha = 1, \ldots, m$ which can be used to accurately represent $|\,\Psi\,\rangle$ as follows

$$|\,\Psi\,\rangle \approx |\,\psi\,\rangle = \sum_{j\alpha} a_{j\alpha} |\,u^\alpha\,\rangle |\,j\,\rangle. \tag{2.4}$$

One way of getting an accurate expansion is to demand that

$$\mathcal{S} = ||\,\Psi\,\rangle - |\,\psi\,\rangle|^2 \tag{2.5}$$

will be minimized by varying over all $a_{j\alpha}$ and $|\,u^\alpha\,\rangle$. It can be shown [5] from linear algebra that the optimal states $|\,u^\alpha\,\rangle$ are the eigenstates of the density matrix ρ of the system AB which are associated to the m largest eigenvalues ω^α of ρ. This can also be explained, or at least hinted at, intuitively. Given the state (or the ensemble) of the superblock $ABCD$ it is possible to construct the so called density operator $\hat{\rho}$ for the system AB

$$\hat{\rho} = \sum_i \omega_i |\,u^i\,\rangle\langle\,u^i\,|, \tag{2.6}$$

where ω_i is the probability of AB to be in the state $|\,u^i\,\rangle$. It is now easy to calculate the probability of AB to be in an arbitrary state $|\,s\,\rangle$

$$P(|\,s\,\rangle) = \langle\,s\,|\hat{\rho}|\,s\,\rangle = \sum_i \omega_i \langle\,s\,|\,u^i\,\rangle\langle\,u^i\,|\,s\,\rangle = \sum_i \omega_i |\langle\,s\,|\,u^i\,\rangle|^2. \tag{2.7}$$

It is at least plausible that the expression in (2.7) is maximized by $|\,s\,\rangle = |\,u^\alpha\,\rangle$ where $\omega_\alpha = max\{\omega_i\}$. But the states $|\,u^i\,\rangle$ happen to be the eigenstates of the density matrix ρ associated with the eigenvalues ω_i. Given this, it is clear that the best state to keep is the state corresponding to the largest eigenvalue, the second best[7] is the state corresponding to the next largest eigenvalue and so on. Thus the density matrix tells us which states are the most important ones.

Suppose that the superblock is in a pure state[8] (2.3). In this case[9] the reduced density matrix for the block AB can be written as

[6] Note that $|\,i\,\rangle|\,j\,\rangle \equiv |\,i\,\rangle \otimes |\,j\,\rangle$.

[7] In the case when only orthogonal states are considered. It is of course just a matter of taste which m states one projects on as long as they span the same subspace as $\{|\,u^\alpha\,\rangle\}$.

[8] I.e. the superblock is certain to be in a quantum state $|\,\Psi\,\rangle$.

[9] This is actually assumed to be the case in all applications in this thesis.

$$\rho_{ij} = \sum_k \psi^*_{ik}\psi_{jk}, \tag{2.8}$$

where ψ_{ik} are the coefficients in (2.3). A more general expression for the density matrix, valid when the superblock is not in a pure state, is

$$\rho_{ij} = \sum_\delta w_\delta \sum_k \psi^{\delta *}_{ik}\psi^\delta_{jk}; \tag{2.9}$$

where w_δ is the probability that the superblock is in the state $|\,\Psi^\delta\,\rangle$.

After ρ has been diagonalized it is easy to form the truncation matrices O. Just as in the case of the standard method the truncation procedure can be written as

$$H_{A'} = OH_{AB}O^\dagger. \tag{2.10}$$

However, this time the rows of O are the states $|\,u^\alpha\,\rangle$ corresponding to the m largest eigenvalues of ρ. This approach does of course also obey the variational principle

$$E_{DMRG} \geq E_0. \tag{2.11}$$

2.3 Infinite systems

There are two different ways to implement the DMRG algorithm. The infinite method in which the system size is increased in every iteration and the finite method where the size of the system is held fixed and the iterations are performed to increase the precision of the calculations. Only the infinite method is discussed and used in this thesis.

2.3.1 The algorithm

The algorithm is in general quite abstract and therefore an example of the method is provided in section 3.3 to make the ideas more transparent. In the following we provide the main steps in a fairly general algorithm for a one-dimensional system with reflection symmetry with respect to the center of the system.

Step 1

Construct four initial blocks A, B, C and D and set up matrices representing the block Hamiltonians and other operators. At this stage the superblock consists of the four initial blocks and one usually chooses each initial block to represent a single site just as in figure 2.5.

Figure 2.5: *An initial configuration of the superblock consisting of only four sites.*

Step 2

Form all relevant operators (such as Hamiltonians and spin operators etc) of the composite blocks AB and CD and the Hamiltonian matrix for the superblock $ABCD$. The operators of the blocks AB and CD are formed from the operators of A, B and C, D respectively and from these one can form the superblock Hamiltonian H_{ABCD}. Note that for systems with reflection symmetry the block CD is just the reflection of AB. In particular when only one site is added in each iteration we get a very simple configuration as shown in figure 2.6.

Figure 2.6: *The configuration of the superblock in the case of systems with reflection symmetry and where only one site is added in each iteration.*

Step 3

Diagonalize the superblock Hamiltonian to find a target state $\Psi_{i_1 i_2 i_3 i_4}$, where i_1 numbers the states of block A and i_2 the states of B etc. In most applications Ψ is the ground state. At this stage it is possible to measure expectation values of various operators expressed in the superblock basis using

$$\langle Q \rangle \equiv \langle \Psi | Q | \Psi \rangle = \sum_{i_1 i_2 i_3 i_4 i_1'} \Psi^*_{i_1 i_2 i_3 i_4} [Q]_{i_1 i_1'} \Psi_{i_1' i_2 i_3 i_4}, \tag{2.12}$$

for an operator Q acting on block A. The formulas for the expectation values of operators on the other blocks are of course similar to (2.12).

Step 4

Form the density matrix for the two-block system AB using

$$\rho_{i_1 i_2 i_1' i_2'} = \sum_{i_3 i_4} \Psi^*_{i_1 i_2 i_3 i_4} \Psi_{i_1' i_2' i_3 i_4}. \tag{2.13}$$

At this stage it is possible to measure expectation values of operators Q acting on the system AB from the relation

$$\langle Q \rangle = Tr \rho Q. \tag{2.14}$$

Step 5

Diagonalize ρ and discard all eigenvectors $|\, u^\alpha \,\rangle$ but the ones associated with the m largest eigenvalues $\omega_\alpha,\ \alpha = 1, \ldots, m$. At this stage it is possible to estimate the truncation error because it corresponds to the deviation of

$$P_m = \sum_\alpha w_\alpha \tag{2.15}$$

from unity. If P_m happens to equal unity then the truncation error is zero.

Step 6

Form a new block A' by changing basis and truncating to m states according to

$$Q_{A'} = O Q_{AB} O^\dagger \tag{2.16}$$

etc, where the rows of O are the chosen density matrix eigenvectors $|\, u^\alpha \,\rangle$, for all the operators Q of the system AB. These are the effective matrix representations of the operators for the new block A'.

Step 7

Replace the old block A with the new block A' and the new block D with the reflection of A'. This is shown in figure 2.7.

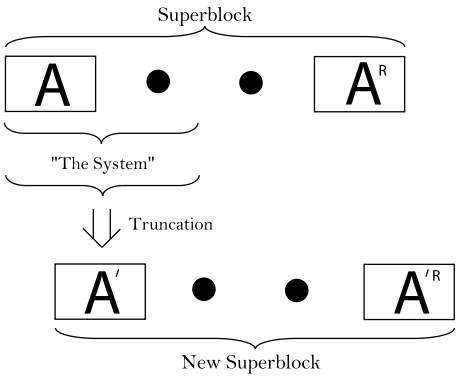

Figure 2.7: *Iteration procedure for systems with reflection symmetry and where only one site is added in every iteration.*

Step 8

Return to step 2.

2.3.2 Measurements

As we have already seen it is fairly easy to measure expectation values of arbitrary, rather complicated, operators on the system or the superblock according to

$$\langle\, Q \,\rangle = Tr\rho Q \tag{2.17}$$

and

$$\langle\, P \,\rangle = \sum_{i_1 i_2 i_3 i_4 i_1'} \Psi^*_{i_1 i_2 i_3 i_4} [P]_{i_1 i_1'} \Psi_{i_1' i_2 i_3 i_4} \tag{2.18}$$

respectively. However it can be costly because all the matrices of the operators that are to be examined have to be stored and updated in a new truncated basis at every iteration. This is of course no problem if one only wants to study a few operators at a time, but if many operators are stored the iterations become slower and one may run out of computer memory. The obvious solution is that one only studies a few operators at a time and that the program is customized for these. When other operators are to be studied one simply rewrites some parts of the DMRG program. One may argue that there are not that many different operators that it would cause problems for most simple systems such as the Heisenberg or Ising chains. But it turns out that it is far more cumbersome to calculate correlation functions.

It is natural to expect that one can calculate expectation values etc of any operator in the system or superblock if one has access to matrices for all possible single-site-operators (such as spin-operators for each site). However this is not the case. If one tries to measure correlation functions such as $\langle\, Q^i P^j \,\rangle$, where i and j denote different sites of the same block[10] in a spin chain, one must be careful since:

$$\langle\, Q^i P^j \,\rangle \neq \sum_{i_1 i_2 i_3 i_4 i_1' i_1''} \Psi^*_{i_1 i_2 i_3 i_4} [Q^i]_{i_1 i_1'} [P^j]_{i_1' i_1''} \Psi_{i_1'' i_2 i_3 i_4}. \tag{2.19}$$

However if j and k are sites on different blocks[11] there is no problem because

$$\langle\, Q^j P^k \,\rangle = \sum_{i_1 i_2 i_3 i_4 i_1' i_4'} \Psi^*_{i_1 i_2 i_3 i_4} [Q^j]_{i_1 i_1'} [P^k]_{i_4 i_4'} \Psi_{i_1' i_2 i_3 i_4'}. \tag{2.20}$$

The reason for this is that the sum over i_1' in (2.19) should, but does not, run over a complete set of states. To be able to measure quantities as the one in (2.19), one has to store (and update at each iteration according to (2.16)) the matrix representations $[Q^i P^j]_{i_1 i_1'}$ throughout the calculation. By doing this it is possible to calculate the expectation value according to

$$\langle\, Q^i P^j \,\rangle = \sum_{i_1 i_2 i_3 i_4 i_1'} \Psi^*_{i_1 i_2 i_3 i_4} [Q^i P^j]_{i_1 i_1'} \Psi_{i_1' i_2 i_3 i_4}. \tag{2.21}$$

An alternative way of looking at this is to consider matrix elements. In fact matrix elements of different operators, expressed in different bases, are all that we have access to during the DMRG calculations. Let $|\, A, B \,\rangle \equiv |\, A \,\rangle \otimes |\, B \,\rangle$ be a state of the block AB. If Q^i operates only on A and P^k operates only on B it is clear that we can write

$$\langle\, A', B' \,|Q^i P^k|\, A, B \,\rangle = \langle\, A' \,|Q^i|\, A \,\rangle \langle\, B' \,|P^k|\, B \,\rangle. \tag{2.22}$$

[10] In equation (2.19) we assume that the block is A.

[11] In equation (2.20) we assume that the blocks are A and D.

From (2.22) it is obvious that we only need to have access to the matrix representations of the single-site-operators in this case. However if both Q^i and P^k operate on the same site, say A, we need a matrix representation for the correlation function since

$$\langle\, A', B' \,|Q^i P^k|\, A, B \,\rangle = \langle\, A' \,|Q^i P^k|\, A \,\rangle \langle\, B' \,|\, B \,\rangle = \delta_{BB'} \langle\, A' \,|Q^i P^k|\, A \,\rangle. \quad (2.23)$$

This fact turns out to severely limit the possibilities of applying DMRG to long range interactions because the Hamiltonians will generally contain terms consisting of such correlation functions discussed above. As we shall see later, in chapter four, these terms do not only exist, but the number of them becomes enormous as the length of the interaction is increased.

Chapter 3

Spin Chains and Model Hamiltonians

As mentioned previously there is a need for simplification in many areas of physics and therefore one must try to find effective theories which are represented by model Hamiltonians. Three such models - the Heisenberg, XY and Ising models - are presented and discussed briefly in this chapter. Furthermore a description of how to apply DMRG to these systems and some results of our own DMRG calculations are included. However, first of all we need a description of the quantum mechanical concept of spin.

3.1 Spin

In classical mechanics a rigid body is often said to have two kinds of angular momentum[1]. Orbital angular momentum ($\overrightarrow{L} = \overrightarrow{r} \times \overrightarrow{p}$) associated with the motion of the center of mass, and spin ($\overrightarrow{S} = \mathbf{I} \cdot \overrightarrow{\omega}$) associated with motion about the center of mass. However this distinction is just a matter of convenience because $\overrightarrow{S}$ is nothing but the sum of all orbital angular momenta of all parts of the body that circle around the center of mass.

In quantum mechanics[2] there is a fundamental distinction between $\overrightarrow{S}$ and $\overrightarrow{L}$. The orbital angular momentum has a similar structure[3] as in classical mechanics. The spin however has no analog in the classical theory since it cannot be thought of as being made up by the angular momentum of constituent parts. A fundamental difference, between $\overrightarrow{L}$ and $\overrightarrow{S}$, that arises in quantum mechanics (QM) is that the spin can have both integer and half integer values while only integer values of the orbital angular momentum are allowed.

The quantum mechanical operator[4] $\vec{S}_i = (S_i^x, S_i^y, S_i^z)$ operates on site i and

[1] This is nicely described in chapter three of Scheck's book [8].

[2] See Sakurai [6] for a more detailed description of spin and angular momentum in QM.

[3] Just let $(x_1, x_2, x_3) \rightarrow (\hat{x}_1, \hat{x}_2, \hat{x}_3)$, $(p_1, p_2, p_3) \rightarrow (\hat{p}_1, \hat{p}_2, \hat{p}_3)$ and impose the canonical commutation relations $[\hat{x}_i, \hat{p}_j] = i\hbar\delta_{ij}$ for the components. The quantum mechanical operators are then obtained as $\hat{L}_i = \sum_{jk} \epsilon_{ijk} \hat{x}_j \hat{p}_k$.

[4] The operator hats are not explicitly written out when there is no risk for confusion.

the components are Hermitian[5] operators which obey the SU(2) algebra

$$[S_i^k, S_j^l] = i\hbar\delta_{ij}\sum_m \epsilon_{klm} S_j^m. \tag{3.1}$$

It is convenient to specify eigenkets of $\vec{S}^2$ and S^z

$$\vec{S}^2|\, s,m\,\rangle = \hbar^2 s(s+1)|\, s,m\,\rangle \tag{3.2}$$
$$S^z|\, s,m\,\rangle = \hbar m|\, s,m\,\rangle. \tag{3.3}$$

With use of these definitions it is now possible to construct ladder operators $S^{\pm} = S^x \pm iS^y$ and it is not hard to figure out how they act on the basis vectors[6]:

$$S^{\pm}|\, s,m\,\rangle = \hbar\sqrt{s(s+1) - m(m\pm 1)}\;|\, s,m\pm 1\,\rangle. \tag{3.4}$$

Observations in nature tell us that every elementary and composite particle has a specific value of spin, s. π-mesons have spin 0; electrons have spin $1/2$; photons have spin 1; Δ-particles have spin $3/2$; gravitons have spin 2 and so on. There is a remarkable connection between the spin of a particle and the statistics it obeys. The half integer ($s = \frac{1}{2}, \frac{3}{2}, \ldots$) spin particles are fermions and they obey the Pauli exclusion principle[7] and Fermi-Dirac statistics. The integer ($s = 0, 1, \ldots$) spin particles obey a fundamentally different kind of statistics, Bose-Einstein statistics, where the particles favor to be in the same state. In non-relativistic QM this has to be taken as an empirical postulate. However, in the framework of relativistic quantum mechanics it can be proved[8] that the half integer spin particles are fermions and that the integer spin particles are bosons.

We are now in a position to list the possible values of the spin s and the z-component m of the spin:

$$s = 0, \frac{1}{2}, 1, \frac{3}{2}, \ldots; \qquad m = -s, -s+1, \ldots, s-1, s. \tag{3.5}$$

In many applications there is no confusion about the spin s of the particles and therefore that index is dropped. For a spin $1/2$ particle we write the two possible states simply as $|\, \frac{1}{2}\,\rangle$ and $|\, -\frac{1}{2}\,\rangle$ or as $|\, \uparrow\,\rangle$ and $|\, \downarrow\rangle$. From this we can easily write down kets of more than one particle by just specifying their m values. Such a ket may for example be written like $|\, \downarrow\downarrow\uparrow\downarrow\uparrow\,\rangle$ for a system of five spin $1/2$ particles.

3.2 The Heisenberg, XY and Ising models

In this section we treat three closely related models, which deal with interacting spin systems. We begin with the most complex one, the Heisenberg model, and

[5] A quantum mechanical operator Q is said to be Hermitian if $Q = Q^\dagger$. $\dagger$ means that $Q^\dagger_{ij} = Q^*_{ji}$ if the operator is expressed in matrix form.

[6] The only assumption needed to prove this is that the eigenkets are properly normalized i.e. $\langle\, s,m'\,|\, s,m\,\rangle = \delta_{m'm}$.

[7] The Pauli exclusion principle states that two fermions cannot occupy the same quantum mechanical state at the same time.

[8] This is shown in [9] for the important special cases of $s = 0, \frac{1}{2}$ and 1.

Figure 3.1: *A qualitative picture of the structure of ferromagnets (left) and antiferromagnets (right).*

then impose constraints which lead to the other two models.

3.2.1 The Heisenberg model

The Heisenberg model is a rather realistic model which describes magnetic systems as interacting spin systems. It was introduced in 1926 by Werner Heisenberg [10] and it leads to parallel or antiparallel spin ordering at low temperatures[9]. At higher temperatures the spin system will of course be in a disordered phase.

One can motivate the form of the Hamiltonian by generalizing the results from a simple system of just two spins with

$$H_{12} = -J\vec{S_1} \cdot \vec{S_2} \tag{3.6}$$

where J is the exchange coupling constant. A negative J Hamiltonian is called antiferromagnetic (AFM), since it favors antiparallel spins, while a positive J Hamiltonian is called ferromagnetic (FM) since its ground state has parallel spins. If one only takes the interaction between nearest neighbors into account the straightforward extension of (3.6) to an N-particle system is

$$H = -J \sum_{\langle i,j \rangle} \vec{S_i} \cdot \vec{S_j} \tag{3.7}$$

which is the so called Heisenberg Hamiltonian[10], where $\langle i, j \rangle$ means that the summation is to be taken over pairs of nearest neighbors only. In this thesis we present results for the one-dimensional version of (3.7). It becomes

$$H = -J \sum_{i=1}^{N-1} \vec{S_i} \cdot \vec{S}_{i+1}. \tag{3.8}$$

To be able to do calculations it is useful to rewrite the scalar product using

$$\vec{S_i} \cdot \vec{S_j} = S_i^z S_j^z + \frac{1}{2}(S_i^+ S_j^- + S_i^- S_j^+). \tag{3.9}$$

The Heisenberg model may seem simple but the solution of the antiferromagnetic chain is extremely complicated and it is only solved for the s=1/2 case in one-dimension. The exact 1-D solution[11] is obtained by use of the Bethe ansatz [11]

[9] The one-dimensional AFM Heisenberg chain is disordered at finite temperatures.

[10] To study the system in a magnetic field just add the term $\sum_i \vec{B} \cdot \vec{S_i}$.

[11] See [13] for the solution. A nice and pedagogical introduction to the solution of the problem is given in [14].

and the ground state energy[12] is found to be

$$E_{AFM} = NJ\hbar^2(-\frac{1}{4} + \ln 2). \tag{3.10}$$

The ferromagnetic Heisenberg chain is much simpler and it has a solution, valid in any dimension, for which the ground state have all the spins parallel. The energy becomes

$$E_{FM} = -N\hbar^2 s^2 zJ/2, \tag{3.11}$$

where z is the number of nearest neighbors of a spin.

Of course a number of conditions, like that the next nearest neighbor interactions can be ignored, has to be fulfilled for (3.7) to be reasonable. Nevertheless there are some physical systems[13] that are accurately described by the Heisenberg Hamiltonian.

3.2.2 The XY model

The XY model is obtained by eliminating the z components of the spin interactions from the Heisenberg Hamiltonian. This means that the Hamiltonian can be written as

$$H = -J \sum_{\langle i,j \rangle} (S_i^x S_j^x + S_i^y S_j^y) \tag{3.12}$$

or more conveniently as

$$H = -\frac{J}{2} \sum_{\langle i,j \rangle} (S_i^+ S_j^- + S_i^- S_j^+). \tag{3.13}$$

The advantage of (3.13) compared to (3.12) is that the same algorithms as the one used for the Heisenberg model can be used[14] and that $S_i^+ = (S_i^-)^\dagger$.

The XY model is completely solvable in one-dimension for spin 1/2 and the solution is much simpler than the Bethe ansatz solution for the Heisenberg chain. The model arises when one deals with superfluidity or superconductivity [17].

3.2.3 The Ising model

By further simplification of the spin chain one can obtain the Ising model[15] [12]; in which only one of the spin components is taken into account. The Hamiltonian can then be written as

$$H = -J \sum_{\langle i,j \rangle} S_i^z S_j^z. \tag{3.14}$$

[12] The first one to compute this energy was Lamek Hultén [15], who worked in Stockholm.
[13] The model describes ferromagnetism of magnetic insulators e.g. EuS or EuO [16].
[14] This is done by imposing $S_i^z = 0$ for all i.
[15] The Ising model was in fact not proposed by Ising himself, but he was the first to solve the 1-D model.

This model seems very simple and it is also classical because all the operators S^z commute. Despite its relative simplicity the model is not (yet) solved in three dimensions even though Onsager [18] found the 2-D solution as early as 1944.

3.3 A DMRG example: The Heisenberg model

The excellent results for the one-dimensional Heisenberg chain were one of the early triumphs of the Density Matrix Renormalization Group algorithm. The ground state of the antiferromagnetic $S = 1/2$ Heisenberg chain is highly non-trivial[16], hence it constitutes a good test for the algorithm. Another advantage with this system is that the actual code can be made fairly compact and transparent even for readers that are not used to similar calculations.

3.3.1 Comments on the algorithms

The infinite system method is the one used for the calculations. The starting point is a small system of only four sites representing four spins according to the recipe given in section 2.3.1. This system is the superblock in the first iteration and all the matrix elements of all relevant operators (such as the Hamiltonian and the spin operators) can easily be computed by hand once a convenient basis is chosen. However it is very helpful to think of how all these matrix elements can be computed from tensor products of the one-site-operators and while doing this one has to keep track of what the basis looks like. Once this small system is fully understood it is not hard (in principle) to construct matrix representations of operators for chains of arbitrary size. If the basis is chosen carefully it is possible to simplify the programs to large extent when the reflection symmetry of the system is used. An example where this is used is given is section 3.3.2.

It is also helpful to consider what the individual matrix elements of different operators for a larger block look like. Consider two neighboring blocks A and B of an antiferromagnetic ($J = -1$) Heisenberg chain. The two blocks interact and we find that

$$[H_{AB}]_{i_1 i_2 i'_1 i'_2} = [H_A]_{i_1 i'_1}\delta_{i_2 i'_2} + \delta_{i_1 i'_1}[H_B]_{i_2 i'_2} + \\ +[S^z_r]_{i_1 i'_1}[S^z_\ell]_{i_2 i'_2} + \frac{1}{2}[S^+_r]_{i_1 i'_1}[S^-_\ell]_{i_2 i'_2} + \frac{1}{2}[S^-_r]_{i_1 i'_1}[S^+_\ell]_{i_2 i'_2} \tag{3.15}$$

and

$$[S^z_r]_{i_1 i_2 i'_1 i'_2} = [S^z_r]_{i_1 i'_1}\delta_{i_2 i'_2} \tag{3.16}$$

etc. The new tensors, with four indices, contain the matrix elements of the operators for the composite block AB. In the next section we go on to show how this is carried out in practice for the antiferromagnetic Heisenberg chain.

3.3.2 The first DMRG steps for the Heisenberg chain

In this section we provide an example of how the calculations for the Heisenberg $S = 1/2$ chain are performed. We start our calculations by constructing

[16] The exact solution, obtained by the Bethe ansatz [11, 15], is very complicated to use, as the reader can check by studying [14].

an initial superblock consisting of four sites as in figure 3.2.

Figure 3.2: *The initial configuration of the superblock of four sites representing ABCD.*

Now we turn our attention to the formation of relevant operators. In order to do this we start by choosing a single particle basis:

$$|1\rangle \equiv |\uparrow\rangle = \begin{pmatrix} 1 \\ 0 \end{pmatrix}; \quad |2\rangle \equiv |\downarrow\rangle = \begin{pmatrix} 0 \\ 1 \end{pmatrix}. \tag{3.17}$$

We can now express the needed single particle operators in matrix form as

$$S^z = \begin{pmatrix} \frac{1}{2} & 0 \\ 0 & -\frac{1}{2} \end{pmatrix}; \quad S^+ = \begin{pmatrix} 0 & 1 \\ 0 & 0 \end{pmatrix}; \quad S^- = \begin{pmatrix} 0 & 0 \\ 1 & 0 \end{pmatrix}, \tag{3.18}$$

where we have put $\hbar = 1$. To be able to form the operators of the block AB, which consists of two sites, we must pick a basis for this system. The natural choice is the direct products of the single site states:

$$\begin{aligned} |1\rangle \equiv |\uparrow\rangle \otimes |\uparrow\rangle = |\uparrow\uparrow\rangle, \quad |2\rangle \equiv |\uparrow\rangle \otimes |\downarrow\rangle = |\uparrow\downarrow\rangle, \\ |3\rangle \equiv |\downarrow\rangle \otimes |\uparrow\rangle = |\downarrow\uparrow\rangle, \quad |4\rangle \equiv |\downarrow\rangle \otimes |\downarrow\rangle = |\downarrow\downarrow\rangle. \end{aligned} \tag{3.19}$$

We can now compute the matrices of the relevant operators acting on AB. This is done with the help of tensor products. From equation (3.6) we obtain the Hamiltonian[17] for the two-spin system AB:

$$H_{12} = S_1^z \otimes S_2^z + \frac{1}{2}(S_1^+ \otimes S_2^- + S_1^- \otimes S_2^+). \tag{3.20}$$

In matrix form we get

$$\begin{aligned} H_{12} = \begin{pmatrix} \frac{1}{4} & 0 & 0 & 0 \\ 0 & -\frac{1}{4} & 0 & 0 \\ 0 & 0 & -\frac{1}{4} & 0 \\ 0 & 0 & 0 & \frac{1}{4} \end{pmatrix} + \frac{1}{2}\begin{pmatrix} 0 & 0 & 0 & 0 \\ 0 & 0 & 1 & 0 \\ 0 & 0 & 0 & 0 \\ 0 & 0 & 0 & 0 \end{pmatrix} + \\ + \frac{1}{2}\begin{pmatrix} 0 & 0 & 0 & 0 \\ 0 & 0 & 0 & 0 \\ 0 & 1 & 0 & 0 \\ 0 & 0 & 0 & 0 \end{pmatrix} = \begin{pmatrix} \frac{1}{4} & 0 & 0 & 0 \\ 0 & -\frac{1}{4} & \frac{1}{2} & 0 \\ 0 & \frac{1}{2} & -\frac{1}{4} & 0 \\ 0 & 0 & 0 & \frac{1}{4} \end{pmatrix} \end{aligned} \tag{3.21}$$

Because of the interaction of the block AB with the block CD we must also form the spin matrices of the rightmost site[18] in the basis of AB. This is done according to

[17] Here we study the antiferromagnetic chain and we set J=-1.

[18] In this case site B.

$$[S_2^z]_{AB} = [\delta_1]_A \otimes [S_2^z]_B \tag{3.22}$$

etc. We are now in a position to write down the Hamiltonian for the superblock:

$$\begin{aligned} H_{ABCD} = H_{12} \otimes \delta_{34} + \delta_{12} \otimes H_{34} + [S_2^z]_{AB} \otimes [S_3^z]_{CD} + \\ + \frac{1}{2}([S_2^+]_{AB} \otimes [S_3^-]_{CD} + [S_2^-]_{AB} \otimes [S_3^+]_{CD}). \end{aligned} \tag{3.23}$$

Taking advantage of the fact that the Heisenberg spin chain has a reflection symmetry[19] we find that we can use the same matrices for H_{34} as for H_{12} and $[S_2^\alpha]_{AB}$ as for $[S_3^\alpha]_{CD}$ where $\alpha = z, +, -$. We can also take advantage of the fact that $S_i^+ = (S_i^-)^\dagger$.

The superblock Hamiltonian, which is a 16×16 matrix, is now diagonalized and we obtain the ground state $|\,\Psi\,\rangle$ and the corresponding energy $E_0 \approx -1,616\ldots$. From $|\,\Psi\,\rangle$ we form the density matrix for AB using (2.13):

$$\rho \approx \begin{pmatrix} 0.0223 & 0 & 0 & 0 \\ 0 & 0.4777 & -0.4553 & 0 \\ 0 & -0.4553 & 0.4777 & 0 \\ 0 & 0 & 0 & 0.0223 \end{pmatrix}. \tag{3.24}$$

In this example we keep $m = 3$ states so we diagonalize the density matrix ρ and keep the three eigenvectors $|\,u^\alpha\,\rangle$ corresponding to the three largest eigenvalues ω_α. These eigenvectors are

$$|\,u^1\,\rangle \approx \begin{pmatrix} 0.0000 \\ -0.7071 \\ 0.7071 \\ 0.0000 \end{pmatrix},\ |\,u^2\,\rangle \approx \begin{pmatrix} -0.5499 \\ 0.3940 \\ 0.3940 \\ -0.6222 \end{pmatrix},\ |\,u^3\,\rangle \approx \begin{pmatrix} 0.8076 \\ 0.1164 \\ 0.1164 \\ -0.5663 \end{pmatrix} \tag{3.25}$$

and the eigenvalues are

$$\omega_1 \approx 0.9330, \quad \omega_2 \approx 0.0223, \quad \omega_3 \approx 0.0223. \tag{3.26}$$

The fourth (discarded) eigenvector $|\,u^4\,\rangle$ happened to have almost the same eigenvalue, $\omega_4 \approx 0.0223$, as two of the kept eigenvectors. So our choice of states to keep could (almost) equally well have been any other set as long as $|\,u^1\,\rangle$ is kept[20].

We now form the truncation matrix O, where the rows of O are the three eigenstates $|\,u^\alpha\,\rangle$:

$$O \approx \begin{pmatrix} 0 & -0.7071 & 0.7071 & 0 \\ -0.5499 & 0.3940 & 0.3940 & -0.6222 \\ 0.8076 & 0.1164 & 0.1164 & -0.5663 \end{pmatrix}. \tag{3.27}$$

[19] The block CD is the same as the reflection of AB with respect to the center of $ABCD$.

[20] The difference between ω_4 and ω_2,ω_3 is only 1.0×10^{-11} and 2.5×10^{-11} respectively. This difference is of course negligible because the error made by discarding one of the eigenstates is larger - by nine orders of magnitude!

The next step is to form the new effective matrices for the relevant operators on AB and then rename the block AB as A'; which is then replacing block A and the next iteration can be performed. This procedure is illustrated in figure 3.3.

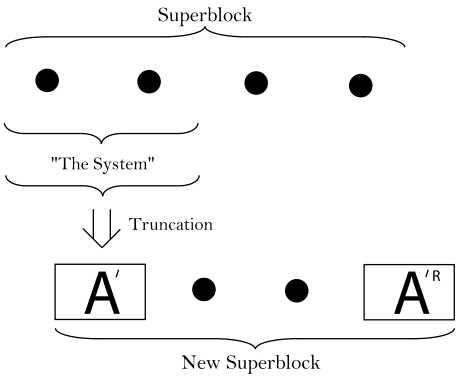

Figure 3.3: *The procedure carried out in the first iteration of our example.*

The truncation of all the operators[21] are of the form of (2.10) and, as an example, we get the following effective Hamiltonian:

$$H_{A'} = OH_{AB}O^{\dagger} \approx \begin{pmatrix} -0,7500 & 0 & 0 \\ 0 & 0,2500 & 0 \\ 0 & 0 & 0,2500 \end{pmatrix}. \qquad (3.28)$$

The observant reader may recognize that we seem to have recovered[22] the singlet state and two of the triplet states. This is expected because in the early iterations the surroundings CD is small[23]. This will however not be the case later in the calculation because CD grows just as fast as AB.

3.3.3 Results

As mentioned earlier the results of DMRG calculations on Heisenberg chains are excellent. In figure 3.4 below, we present the ground state energies as well as the truncation errors of a Heisenberg chain calculation keeping only four states. Even though only four states are kept and the calculation time is just a matter of seconds on an ordinary workstation, the above example shows good precision. As seen in figure 3.4 the ground state energy seems to converge as the length of the system goes to infinity. As a matter of fact an extrapolation of the curve to infinity shows that it approaches a value that differs by about 2.8×10^{-3} from the exact result $E_0 = \frac{1}{4} - \ln 2 = -0.443147\ldots$ obtained by use of the Bethe ansatz [11]. It is also worth noting that this difference is at

[21] To be able to continue the calculations one has to keep, as a minimum, the Hamiltonian H_{AB} as well as the spin operators S_r^z and one of S_r^+ or S_r^-, where r denotes the rightmost site of AB.

[22] If more digits were to be presented in (3.28) it would be clear that it is only a good approximation and not the exact result.

[23] In the limit of no surroundings the DMRG will be equivalent to standard RG and the exact eigenstates of H_{AB} will be kept.

the order of the typical truncation error at each iteration. As the number of states kept, m, is increased the results are naturally improved. In table 3.1 we present some of these results for the infinite $S = 1/2$ Heisenberg chain obtained using our DMRG program, and we illustrate how these results are obtained in figure 3.5. The results are obtained from calculations for $N = 4000$ sites by extrapolating $\frac{1}{N} \to 0$. Furthermore the early iterations have been excluded in these calculations since the surroundings are so small that the calculations may not be reliable.

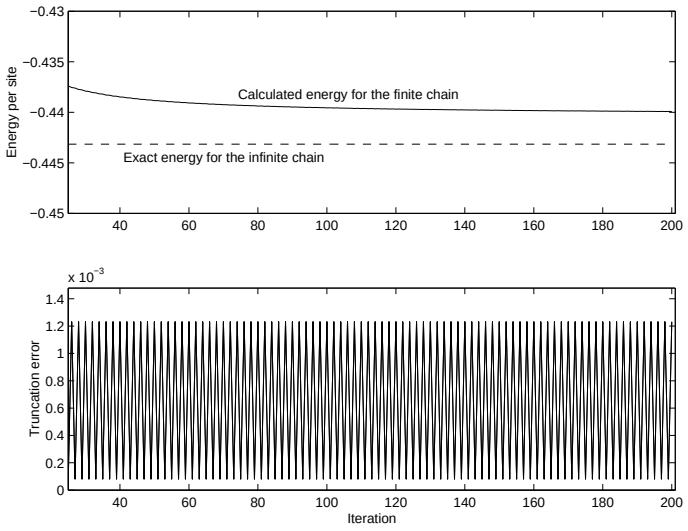

Figure 3.4: *A DMRG calculation of the average ground state energy per site for the antiferromagnetic spin 1/2 Heisenberg chain keeping only four states ($m = 4$). The energy per site (above) is computed from the superblock configuration as a function of the number of iterations and is given in units of $\hbar = 1$. The superblock includes $2i + 2$ sites at the ith iteration. The truncation error (below) at each iteration is given by $1 - P_m = 1 - \sum_{i=1}^{m} \omega_i$.*

m	$E_0^{DMRG} - E_0^{exact}$
4	2.8×10^{-3}
8	3.0×10^{-4}
12	1.5×10^{-4}
16	5.9×10^{-5}
20	2.6×10^{-5}

Table 3.1: *DMRG results for the infinite AFM spin 1/2 Heisenberg chain.*

As seen in table 3.1 the error is falling rapidly with increasing m. It is of course just a matter of computer time to get even better results. However, one should keep in mind that one has to diagonalize a $4m^2 \times 4m^2$ matrix for the superblock in every iteration, so the iterations become very time consuming for large m.

We have also done calculations on the XY and Ising models, but these results are not presented because we want to keep this thesis short and also because these results are easier[24] to obtain[25] using other methods such as the standard Renormalization Group or Monte Carlo simulations.

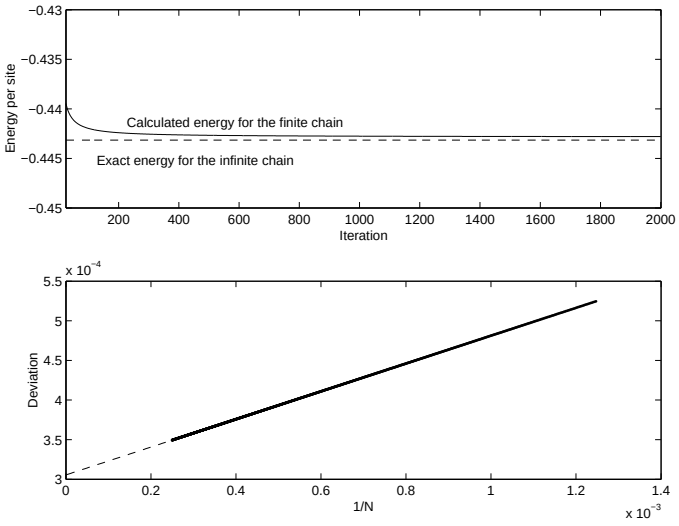

Figure 3.5: *An illustration of how the results in table 3.1 are obtained. The full line correspond to calculated deviations from the exact infinite chain ground state energy and the dashed line represents the extrapolated curve. We kept eight states in each iteration in this particular example.*

[24] This is particulary true for the Ising model.
[25] Compared to the Heisenberg results.

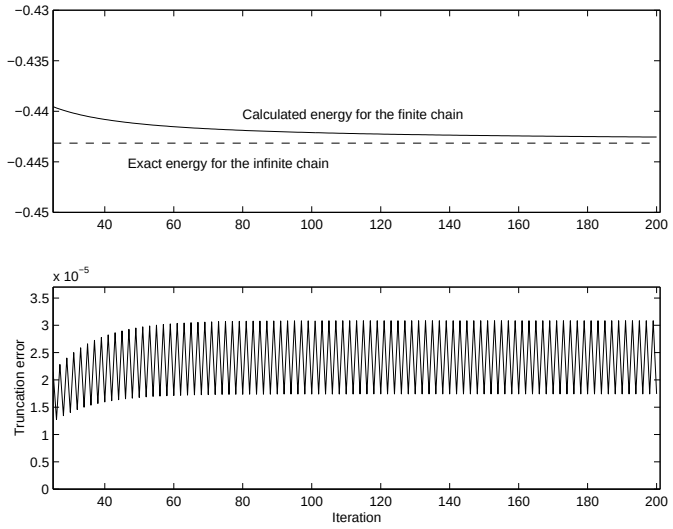

Figure 3.6: *A DMRG calculation of the ground state energy for the antiferromagnetic spin 1/2 Heisenberg chain keeping twelve states. Compared to the results in figure 3.4, the truncation error is much smaller and the energy is closer to the exact value for the infinite chain.*

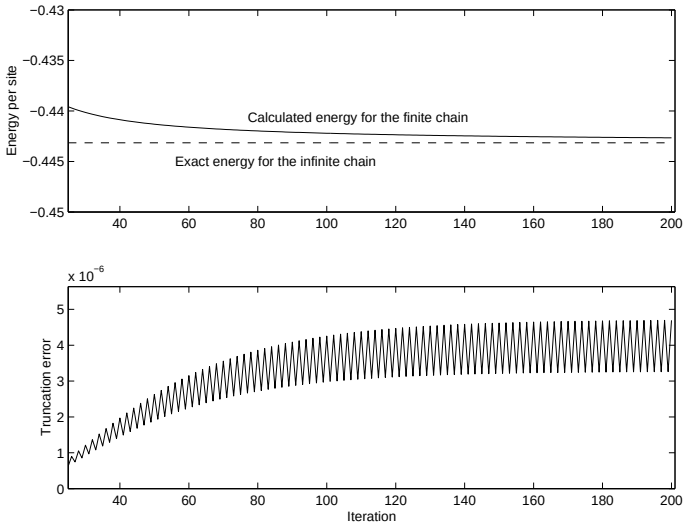

Figure 3.7: *A DMRG calculation of the groundstate energy for the AFM spin 1/2 Heisenberg chain keeping twenty states. The results are now very accurate.*

Chapter 4

Application to Quantum Hall Systems

In this chapter we apply the ideas of DMRG to a two-dimensional system with longer ranged interactions. This system is a quantum Hall system[1] consisting of a two-dimensional electron gas on a cylinder with a strong magnetic field perpendicular to the electron layer.

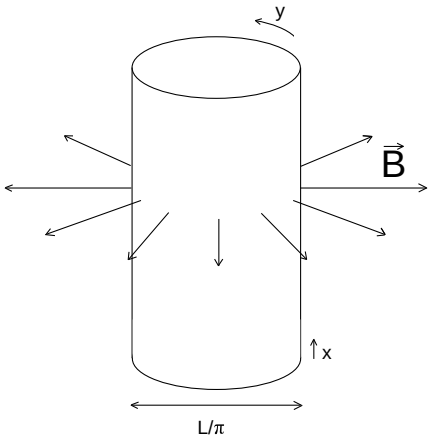

Figure 4.1: *A cylinder with a magnetic field $\vec{B}$ perpendicular to the electron layer.*

Quantum Hall systems are of course more complicated than the one-dimensional systems studied in chapter three. Hence we need to generalize the methods we used for the spin chains. There are two big differences that have to be taken care of: 1) the system is now two-dimensional and 2) the interaction is long range instead of only between nearest neighbors.

The first problem is handled by mapping the two-dimensional system onto a

[1] See Girvin [19] for a good review.

set of one-dimensional harmonic oscillators. This is done in section 4.1. The longer range generalization is discussed in section 4.2 and in section 4.3 we implement these ideas in our DMRG calculations.

In order to accomplish our task we first study the single particle states and thereafter we take the interaction into account. From the interaction and the single particle states we find a second quantized form of the Hamiltonian. The Hamiltonian is then analyzed and the ground states are approximated by use of the DMRG method.

4.1 Quantum mechanics in strong B-fields

In this section we study the quantum states of a single electrically charged particle in a two-dimensional system with a perpendicular magnetic field. Such a system is illustrated by figure 4.1 and the states we seek correspond to the states where just one particle is present on the surface of the cylinder.

In order to find the single particle Hamiltonian we use the concept of minimal coupling and choose an appropriate gauge for the vector potential. A good choice is the so-called Landau gauge:

$$\vec{A} = Bx\hat{y} \tag{4.1}$$

which gives a magnetic field in the direction of $\hat{z}$ because $\nabla \times \vec{A} = B\hat{z}$. We can now write the Hamiltonian as

$$H = \frac{1}{2m}(p_x^2 + (p_y + \frac{eB}{c}x)^2) \tag{4.2}$$

using minimal coupling. As one can see from this expression the Hamiltonian is not invariant under translation along the $\hat{x}$-axis, even though the physics is (B-field only in the $\hat{z}$-direction).

Let us now consider this system on a cylinder as shown in figure 4.1. We take advantage of the translation symmetry in the $\hat{y}$-direction and write the wave function as

$$\psi(x, y) = e^{iky}\xi(x) \tag{4.3}$$

where we have used separation of variables as an ansatz. Written in this form it is an eigenstate of p_y and hence we can make the substitution $p_y \to \hbar k$ in the Hamiltonian. The system also gives us a constraint on k. Imposing periodic boundary conditions

$$\psi_k(x, y) = \psi_k(x, y + L) \tag{4.4}$$

gives

$$k = \frac{2\pi p}{L}, \quad p = 0, \pm 1, \ldots \tag{4.5}$$

where L is the circumference of the cylinder. We then arrive at an effective one-dimensional Schrödinger equation

$$h_k\xi(x) = \epsilon_k\xi(x) \tag{4.6}$$

where

$$h_k \equiv \frac{1}{2m}(p_x^2 + (\hbar k + \frac{eB}{c}x)^2). \tag{4.7}$$

This is a familiar equation, namely the one-dimensional harmonic oscillator. We can therefore use our knowledge from elementary quantum mechanics [6]. The eigenvalues are

$$\epsilon_n = (n + 1/2)\hbar\omega_c, \qquad n = 0, 1, \ldots \tag{4.8}$$

where $\omega_c \equiv \frac{eB}{mc}$ is the cyclotron frequency. The corresponding eigenfunctions[2] are

$$\psi_{nk}(\vec{r}) = \frac{1}{\sqrt{\pi^{1/2}2^n n! L}} e^{iky} H_n(x + k\ell^2) e^{-\frac{1}{2\ell^2}(x+k\ell^2)^2}, \tag{4.9}$$

where H_n is the nth Hermite polynomial and $\ell \equiv \sqrt{\frac{\hbar c}{eB}}$ is the so-called magnetic length. In this thesis we are only interested in the lowest Landau level ($n = 0$) with the following eigenfunctions:

$$\psi_k(\vec{r}) = \frac{1}{\sqrt{\pi^{1/2} L\ell}} e^{iky} e^{-\frac{1}{2\ell^2}(x+k\ell^2)^2}. \tag{4.10}$$

As we shall se later these eigenfunctions are well suited for the DMRG method.

Equation (4.8) tells us that the number n gives the energy of a single particle state. Since n is an integer it means that there are discrete energy levels, these are the so called Landau levels [20].

From figure 4.2 we see that the area per state in the lowest Landau level is $2\pi\ell^2$, thus the density of states is $n_s = \frac{1}{2\pi\ell^2}$. Given the number of electrons n_e per unit area in the system we can define the filling fraction ν as

$$\nu \equiv \frac{n_e}{n_s} = 2\pi\ell^2 n_e = \frac{2\pi\hbar c}{eB} n_e. \tag{4.11}$$

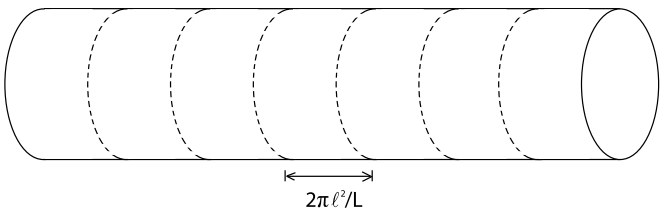

Figure 4.2: *An illustration on how the quantum single particle states are distributed on the cylinder. The dotted lines represent the lines $X_k = -k\ell^2$ around which the states ψ_k are centered.*

[2] Note that the eigenfunctions are centered at $x = X_k = -k\ell^2$, i.e. the single particle wave functions are centered at different x-coordinates depending on the momentum of the state.

4.2 The Hamiltonian

In analogy to the case of the spin chains we need to find a matrix formulation of the Hamiltonian to be able to apply the DMRG methods. We also need to make some simplifications to get a system that the computers of today can handle.

4.2.1 Instead of the Coulomb interaction

That the Coulomb interaction has infinite range means that there will be problems for the algorithms when large systems are studied. In fact the problems will be enormous because when the size of the system goes to infinity so does the number of matrices that one has to keep in every iteration and therefore the size of the code also diverges. Unfortunately the Coulomb interaction

$$V(\vec{r}) = \frac{e^2}{4\pi\epsilon|\vec{r}|} \tag{4.12}$$

does not vanish fast enough for our purposes. Therefore a more local interaction is introduced. Trugman and Kivelson [21] proposed that the interaction can be expanded as

$$V(\vec{r}) = \sum_j c_j b^{2j} \nabla^{2j} \delta^2(\vec{r}), \tag{4.13}$$

where b is the range of the interaction. In the limit of short range, $b \to 0$, the expression (4.13) reduces to

$$V(\vec{r}) = c_1 b^2 \nabla^2 \delta^2(\vec{r}) \tag{4.14}$$

since $\langle\, \delta^2(\vec{r}) \,\rangle = 0$ for any antisymmetric state. The form of this interaction can be motivated [21] by the fact that the physics of quantum Hall systems does not change significantly if the interaction is made more local. Furthermore the Laughlin states [2] can in fact be shown to be exact eigenstates of this particular interaction. Expressed in complex coordinates $z = x + iy$ the Laughlin wave function is

$$\Psi_{\frac{1}{2m+1}}(z_1, z_2, \ldots, z_N) = \prod_{i<j}(z_i - z_j)^{2m+1} \prod_i e^{-\frac{1}{4}|z_i|^2/\ell^2}. \tag{4.15}$$

This describes the quantized Hall states at filling fraction $\nu = \frac{1}{2m+1}$ in a circular geometry. At $\nu = \frac{1}{2m}$ the Fermi liquid like states are observed. They are described by wave functions obtained from $\nu = \frac{1}{2m}$ Laughlin states. One forms an antisymmetric state while doing as little damage as possible to the Laughlin state. This is done by multiplying with a determinant[3]. One gets

$$\Psi_{\frac{1}{2m}}(z_1, z_2, \ldots, z_N) = \mathcal{P}_{LLL} Det[e^{i\mathbf{k}_i \cdot \mathbf{r}_j}] \prod_{i<j}(z_i - z_j)^{2m} [\prod_i e^{-\frac{1}{4}|z_i|^2/\ell^2}], \tag{4.16}$$

which is the so called Rezayi-Read [23] wave function where $\mathcal{P}_{LLL}$ is a projection operator which projects the state onto the lowest Landau level.

[3] See [22] for a more complete discussion of the properties of these states.

4.2.2 Second quantized form of the Hamiltonian

Inspired by previous attempts with momentum space methods for DMRG [24, 25] we look for a suitable form of the Hamiltonian. Let us introduce creation and annihilation operators[4] $c^\dagger$ and c respectively and impose anti-commutation[5] relations:

$$\{c_i^\dagger, c_j\} \equiv c_i^\dagger c_j + c_j c_i^\dagger = \delta_{ij} \tag{4.17}$$

and

$$\{c_i, c_j\} = \{c_i^\dagger, c_j^\dagger\} = 0. \tag{4.18}$$

We then get the following expression for the second quantized Hamiltonian:

$$H = \frac{1}{2} \sum_{klmn} V_{klmn} c_k^\dagger c_l^\dagger c_m c_n \tag{4.19}$$

where

$$V_{klmn} = \int\int \psi_k^\dagger(\vec{r}) \psi_l^\dagger(\vec{r}') V(\vec{r} - \vec{r}') \psi_m(\vec{r}') \psi_n(\vec{r}) d^2r d^2r' \tag{4.20}$$

with the eigenfunctions ψ_k from (4.10). We can now compute the matrix elements (4.20) using the interaction (4.14) and the eigenfunctions in (4.10). Since we are dealing with infinite systems in this thesis we simply let the height of the cylinder in figure 4.1 go to infinity. We set[6] $\ell = 1$ and find that

$$\begin{aligned} V_{klmn} &= \int\int d^2r d^2r' [\psi_k^\dagger(\vec{r}) \psi_l^\dagger(\vec{r}')][c_1 b^2 \nabla_{r-r'}^2 \delta^2(\vec{r} - \vec{r}')] \psi_m(\vec{r}') \psi_n(\vec{r})] \\ &= \frac{c_1 b^2}{\pi L^2} \int_{-L/2}^{L/2} \int_{-\infty}^{\infty} \int_{-L/2}^{L/2} \int_{-\infty}^{\infty} dx\ dy\ dx'\ dy' [(\partial_{x-x'}^2 + \partial_{y-y'}^2)\delta(x - x')\delta(y - y') \\ &\qquad \times e^{i(n-k)y - \frac{1}{2}((x+k)^2 + (x+n)^2)} e^{i(m-l)y' - \frac{1}{2}((x'+l)^2 + (x'+m)^2)}] \\ &= \frac{c_1 b^2}{\sqrt{2\pi} L} \delta_{k+l,m+n} ((n-l)^2 - (n-k)^2 - 1) e^{kl - \frac{1}{2}(m^2+n^2)}. \end{aligned} \tag{4.21}$$

From now on we set $c_1 = \frac{2\sqrt{2\pi}L}{b^2}$ in order to get a repulsive interaction and units that are easy to work with. We now note that if $k = l$ (or $m = n$) we will get no contribution. Furthermore we note that only the parts of V_{klmn} that are antisymmetric in $k \longleftrightarrow l$ and $m \longleftrightarrow n$ survive in the sum due to the anti-commutation relations (4.18). Given this we can write our Hamiltonian as

$$H = \sum_{klmn} (1 - \delta_{kl}) \delta_{k+l,m+n} ((n-l)^2 - (n-k)^2) e^{kl - \frac{1}{2}(m^2+n^2)} c_k^\dagger c_l^\dagger c_m c_n. \tag{4.22}$$

We can easily see from (4.22) that the physics is invariant under translation in momentum space[7]. This means that we only have to calculate a few matrix elements and use them throughout the calculations because we can re-number the sites at each iteration. Furthermore, we note that the matrix elements just

[4] $c_k^\dagger$ creates a fermion with momentum k and c_l annihilate a fermion with momentum l.

[5] The anti-commutation relations assure that the fermion wave functions are antisymmetric under particle exchange.

[6] I.e. we work in units where the magnetic length is the unit length.

[7] To see this just add a constant α to k, l, m, and n, and use the constraint $k + l = m + n$.

depend on two indices and some index-manipulation leads us to the following form of the Hamiltonian

$$H = \sum_n \sum_{k>l} (k^2 - l^2) e^{-\frac{1}{2}(k^2+l^2)} c^\dagger_{l+n} c^\dagger_{k+n} c_{l+k+n} c_n. \tag{4.23}$$

Written in the form (4.23) it is easier to see how the interaction falls with distance and the translation invariance is also made more transparent. However, the expression (4.22) is more convenient when we implement the DMRG algorithm.

Even though a very local interaction is used it is obvious that the interaction never vanishes completely. The solution to this problem is that we introduce a cutoff distance d, in terms of the number of interacting neighbors[8], for the interaction. This means that for distances larger than d the interaction is considered so weak that we just neglect it.

There are a great number of symmetries that can be used to improve the algorithms, but it would not be meaningful to discuss all of them here. However, there are two nice properties of the Hamiltonian that are worth mentioning. By use of the anti-commutation relations (4.17) and (4.18) we can easily derive

$$\begin{aligned} & V_{klmn} c^\dagger_k c^\dagger_l c_m c_n + V_{lknm} c^\dagger_l c^\dagger_k c_n c_m \\ & + V_{klnm} c^\dagger_k c^\dagger_l c_n c_m + V_{lkmn} c^\dagger_l c^\dagger_k c_m c_n \\ = & (V_{klmn} + V_{lknm} - V_{klnm} - V_{lkmn}) c^\dagger_k c^\dagger_l c_m c_n \end{aligned} \tag{4.24}$$

which is valid for all non-vanishing operators appearing in the Hamiltonian (4.19). The expression (4.24) shows that one does not have to calculate as many operators as matrix elements of V. This is of course good news because it is a lot more demanding to compute matrix representations of the operators than it is to compute the matrix elements, since these are just numbers.

In order to further reduce the number of computed operators we use that

$$\begin{aligned} & (c^\dagger_k c_m c_n c^\dagger_l)^\dagger = (c_n c^\dagger_l)^\dagger (c^\dagger_k c_m)^\dagger \\ & = (c^\dagger_l)^\dagger c^\dagger_n c^\dagger_m (c^\dagger_k)^\dagger = c_l c^\dagger_n c^\dagger_m c_k. \end{aligned} \tag{4.25}$$

Since (4.25) is valid for all strings of operators we have reduced the number of needed operators even further.

A special case of (4.24) can be used to study which terms are the important ones in our calculations. We simply gather the matrix elements (4.21) and find that

$$(V_{klmn} + V_{lknm} - V_{klnm} - V_{lkmn}) = -4(k-l)(m-n) e^{kl - \frac{1}{2}(m^2+n^2)}. \tag{4.26}$$

In order to analyze this result we note that the terms where $k - l = m - n$ are the largest ones[9]. Let us look at the coefficient corresponding to interaction

[8] For $d = 1$ we only consider nearest neighbor interactions and for $d = 2$ we also include next nearest neighbor interactions etc.

[9] This is of course only valid when terms corresponding to the same range are compared.

between sites with momentum 0 and k. We conclude that

$$(V_{k0k0} + V_{0k0k} - V_{k00k} - V_{0kk0}) \sim k^2 e^{-k^2/2}. \tag{4.27}$$

We can now see clearly that our interaction, that was constructed in order to be very local, is in fact not maximal for small k. The maximum magnitude is in fact at $k = \sqrt{2}$ and if we consider the expression (4.5) it is clear that we can only handle systems with small L since we cannot handle interactions between sites separated by long distances. In fact we need to specify the cutoff distance d in terms of how many neighbors a given site interacts with, to the left or to the right of the site itself. We can interpret the length of the interaction in momentum space as

$$\Delta k = \frac{2\pi d}{L}. \tag{4.28}$$

Hence we can only treat systems with relatively small circumference L. Typically we are forced to use $L \sim 2\pi$ in order to get reliable results.

4.2.3 Number representation of fermionic states

We need to construct a many particle basis for the Hilbert space in which we can perform our calculations. It is helpful to note that the momentum quantum number of a particle has the same meaning as the number/position of the site had in our calculation for the spin chains. This is natural because, as we saw earlier, the single particle wave functions are centered at positions governed by the momentum. With this in mind we now adopt the name site for a state with a given momentum.

A good basis is the number representation where we start out by defining the vacuum state

$$c_i |\, 0 \,\rangle = 0, \quad i = 1, 2, \ldots, N_s \tag{4.29}$$

where N_s is the maximal possible number of particles in the lowest Landau level. We now act with the creation operators on the vacuum state in order to create particles with a specified momentum

$$c_k^\dagger |\, 0 \,\rangle = |\, 0_1, \ldots, 1_k, \ldots, 0_{N_s} \,\rangle, \quad k = 1, 2, \ldots, N_s. \tag{4.30}$$

A more general state is of course given by

$$|\, n_1, \ldots, n_k, \ldots, n_{N_s} \,\rangle = \prod_{i=1}^{N_s} (c_i^\dagger)^{n_i} |\, 0 \,\rangle. \tag{4.31}$$

These are the basis states which span our 2^{N_s} dimensional Hilbert space[10]. Hence any state can be written as a linear combination of the states (4.31). Since we are dealing with fermions all the occupation numbers $n_i,\ i = 1, 2, \ldots, N_s$, are either zero or one.

[10] A nice property of these states is that if the vacuum is normalized ($\langle\, 0 \,|\, 0 \,\rangle = 1$), so are all the other states.

It is nice to introduce number operators, which indeed justify the name of the representation. We form the operator that counts the number of particles of momentum k as

$$\hat{N}_k \equiv c_k^\dagger c_k \tag{4.32}$$

and an operator that counts the total number of particles:

$$\hat{N}_{total} \equiv \sum_{i=1}^{N_s} \hat{N}_i. \tag{4.33}$$

It is not hard to see that the number representation provides a set of eigenkets of these operators. We get

$$\hat{N}_k |\, n_1, \ldots, n_k, \ldots, n_{N_s} \,\rangle = n_k |\, n_1, \ldots, n_k, \ldots, n_{N_s} \,\rangle, \tag{4.34}$$

and

$$\hat{N}_{total} |\, n_1, \ldots, n_k, \ldots, n_{N_s} \,\rangle = (\sum_{i=1}^{N_s} n_i) |\, n_1, \ldots, n_k, \ldots, n_{N_s} \,\rangle. \tag{4.35}$$

In order to be able to use these results we introduce a matrix representation for the basis states. Just as in the case of the spin chain take

$$|\, 1 \,\rangle = \begin{pmatrix} 1 \\ 0 \end{pmatrix}; \quad |\, 0 \,\rangle = \begin{pmatrix} 0 \\ 1 \end{pmatrix}, \tag{4.36}$$

where $|\, 1 \,\rangle$ and $|\, 0 \,\rangle$ represent the existence and non-existence of a particle with a given momentum, respectively. A many particle state is now straight forwardly given by direct products as

$$|\, n_1, \ldots, n_k, \ldots, n_{N_s} \,\rangle = \begin{pmatrix} n_1 \\ 1-n_1 \end{pmatrix} \otimes \ldots \otimes \begin{pmatrix} n_k \\ 1-n_k \end{pmatrix} \otimes \ldots \otimes \begin{pmatrix} n_N \\ 1-n_{N_s} \end{pmatrix}. \tag{4.37}$$

We now produce a representation of the creation and annihilation operators using this basis. It is easy to see that these matrices do the job for a single site:

$$c^\dagger = \begin{pmatrix} 0 & 1 \\ 0 & 0 \end{pmatrix}; \quad c = \begin{pmatrix} 0 & 0 \\ 1 & 0 \end{pmatrix}. \tag{4.38}$$

We can of course also construct representations of arbitrary composite operators by tensor products of the single site operators in the same manner as we formed the spin operators earlier. An alternative way of getting states as in (4.37) is to first construct single site creation operators, expressed in the many site basis, and then use equation (4.31) to obtain the states from the vacuum state[11]. A further discussion on how relevant operators are formed is given in section 4.3.2.

[11] Which is a simple special case of (4.37) with $n_k = 0$ for all k.

4.3 DMRG

Since the Hamiltonian we investigate in this thesis has a longer interaction range than the nearest neighbor interaction of the spin chains, we are forced to write longer and more intricate computer programs. But we are not facing any new fundamental difficulties.

4.3.1 Ground states for any given density

Because the interactions between the particles are repulsive one naturally expects that the ground state should be the empty state and the highest lying energy state should correspond to a filled state. However it is more interesting to investigate states with a definite number of particles i.e. a definite density. This is motivated by the fact that the physical system as a hole should be electrically neutral, i.e. the electrons are compensated by a positive background charge.

In order to target a state of a specific filling fraction (density), ν , we add an extra term to the Hamiltonian that makes it energetically favorable to be in a state with that density. We also want to find a state with no spread of the density i.e. the mean density of the system should be ν and the standard deviation should be zero. This is natural to demand because we want to target a state of definite density and not a linear combination of other states that happens to give ν when we compute the expectation value of the density. In order to achieve this we introduce a new operator

$$\hat{n} \equiv \frac{1}{N}\sum_{i=1}^{N} c_i^\dagger c_i \tag{4.39}$$

which gives the average density of the system. Now we add an extra term to the Hamiltonian:

$$H \to H' = H + \Delta H = H + \gamma N^2(\hat{n} - \nu)^2 \tag{4.40}$$

where $\nu \in [0, 1]$. This means that we can express ΔH in matrix representation as

$$\Delta H_{ij} = \gamma N^2 \sum_k (n_{ik} - \nu\delta_{ik})(n_{kj} - \nu\delta_{kj}). \tag{4.41}$$

Let us go on to see what this means. Using the definition of the uncertainty of an operator $\Delta\hat{n}$ and the linearity of expectation values we find

$$\begin{aligned}
\langle \Psi | \Delta H | \Psi \rangle = \langle \Delta H \rangle &= \langle \gamma N^2(\hat{n} - \nu)^2 \rangle \\
&= \gamma N^2 \langle \hat{n}^2 - 2\nu\hat{n} + \nu^2 \rangle \\
= \gamma N^2 (\underbrace{\langle \hat{n}^2 \rangle - \langle \hat{n} \rangle^2}_{\equiv(\Delta\hat{n})^2} &+ \langle \hat{n} \rangle^2 - 2\nu\langle \hat{n} \rangle + \nu^2) \\
&= \gamma N^2(\Delta\hat{n})^2 + \gamma N^2(\langle \hat{n} \rangle - \nu)^2.
\end{aligned} \tag{4.42}$$

When γ is large enough the ground state of the new Hamiltonian H' will not be the empty state, but a state which minimizes the contribution from ΔH. However, this contribution is clearly positive semi-definite:

$$\langle\, a \,|\Delta H|\, a \,\rangle \geq 0 \tag{4.43}$$

for all states $|\, a \,\rangle$. This means that the ground state, $|\, \Psi \,\rangle$, of H' will be such that it satisfies

$$\langle\, \Psi \,|\Delta H|\, \Psi \,\rangle = 0. \tag{4.44}$$

This clearly fixes the average density to ν and minimizes the spread in this variable. So we have found a term that accomplishes our task when it is added to the Hamiltonian. There is of course a huge number of possible states that fulfills this condition but the state we find when we minimize $\langle\, \Psi \,|H'|\, \Psi \,\rangle$ with respect to $|\, \Psi \,\rangle$ is naturally also the state that has the lowest energy because of the first term in the expression (4.40) for H'.

4.3.2 Comments on the algorithm

The algorithm for the QH systems is equivalent to the spin chain methods in most parts. However, there are some vital differences due to the fact that the interaction is no longer only between nearest neighbors. The Hamiltonian is built up by operators of the form

$$c_k^\dagger c_l^\dagger c_m c_n \tag{4.45}$$

where k, l, m and n represent either two or four different sites. In the case of two distinct sites we have simple interactions corresponding to operators like

$$c_k^\dagger c_k c_l^\dagger c_l \equiv \hat{N}_k \hat{N}_l. \tag{4.46}$$

The above expression (4.46) just gives the (repulsive) interaction between the particles of momentum k and l and it is easily treated just in the same manner as the spin interactions were treated earlier. The only difference, in this case, is that one has to keep[12] more operators $\hat{N}_k = c_k^\dagger c_k$ because of the increased length of interaction.

In the case when all of k, l, m and n are different we end up with slightly more complicated operators. These are formed in steps by iterative use of tensor products of the single site operators. The following example will probably make the idea more transparent:

Example 1

Suppose that we want to construct the operator

$$c_i^\dagger c_{i+4}^\dagger c_{i+1} c_{i+3} = c_i^\dagger c_{i+1} c_{i+3} c_{i+4}^\dagger. \tag{4.47}$$

Starting from the matrix representation of $c_i^\dagger$ when i is the rightmost site of the block A we add a single site $i+1$ representing B. We get

[12] And of course update to new basis sets.

$$[c_i^\dagger c_{i+1}]_{AB} = [c_i^\dagger]_A \otimes [c_{i+1}]_B. \tag{4.48}$$

This operator is now truncated using

$$[c_i^\dagger c_{i+1}]_{A'} = O[c_i^\dagger c_{i+1}]_{AB} O^\dagger \tag{4.49}$$

and A' is renamed $A' \to A$. We now add another site $i+2$ but this time there is no creation or annihilation operator acting on the site in the expression (4.47). We insert a unit matrix instead:

$$[c_i^\dagger c_{i+1}]_{AB} = [c_i^\dagger c_{i+1}]_A \otimes [\delta_{i+2}]_B. \tag{4.50}$$

This is now truncated and a new representation is obtained;

$$O: \quad [c_i^\dagger c_{i+1}]_{AB} \mapsto [c_i^\dagger c_{i+1}]_{A'}. \tag{4.51}$$

Now A' is renamed $A' \to A$ and the site $i+3$ is added. The new operator

$$[c_i^\dagger c_{i+1} c_{i+3}]_{AB} = [c_i^\dagger c_{i+1}]_A \otimes [c_{i+3}]_B \tag{4.52}$$

is formed. Just as in the previous steps the operator is truncated and in the last step we form

$$[c_i^\dagger c_{i+1} c_{i+3} c_{i+4}^\dagger]_{AB} = [c_i^\dagger c_{i+1} c_{i+3}]_A \otimes [c_{i+4}^\dagger]_B. \tag{4.53}$$

We have now arrived at a representation of one of the operators[13] that form the QH Hamiltonian (4.22).

4.3.3 Results

As already mentioned we are forced to study the quantum states on thin cylinders. Although we have tried to vary the circumference L of the cylinder we decided to only present the results obtained for $L = 2\pi$. Hence the physical system can be interpreted as a very local interaction on a thin but very long cylinder. Furthermore we present results obtained with d ranging from four to six. There are no observed qualitative differences when we use these different interaction lengths.

The results were quite surprising. We expected, or hoped, to find some of the fractional quantum Hall states [2] for the lowest Landau level corresponding to

$$\nu = \frac{1}{2m+1}, \qquad m \in \mathbf{N} \tag{4.54}$$

where m is a positive integer. However these states were not found but instead we seem to have found another interesting state - a homogenous state at $\nu = 1/2$. There are two more states that were easily found. The empty $\nu = 0$ state and the filled $\nu = 1$ state. The structure of these two states is of course trivial but the fact that they are found indicates that our calculations are making sense. Another nice thing that we observed was that the states were totally symmetric in particles $\longleftrightarrow$ holes when $\nu \longleftrightarrow 1-\nu$ for $\nu \leq 1/2$. In

[13] Namely the operator (4.47).

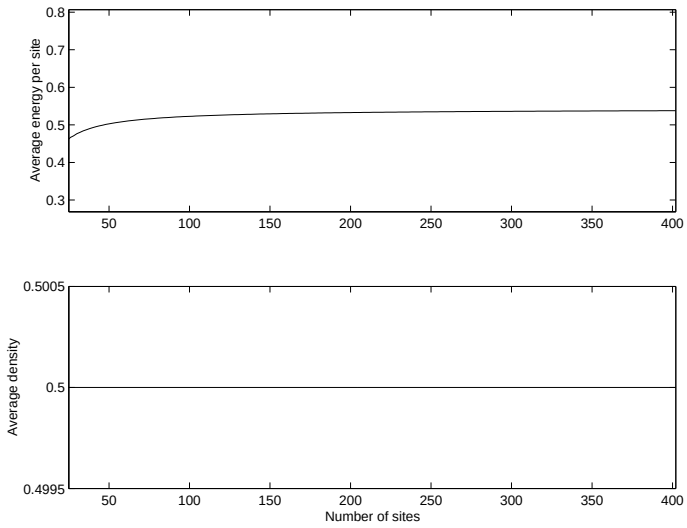

Figure 4.3: *The $\nu = 1/2$ ground state energy per site (above) and the average density of the system (below) obtained with four states kept. The average density is almost perfectly constant and the energy seems to converge smoothly. That the energy increases is due to the fact that the edge effects become less important when the system size is increased.*

figure 4.3 we present results obtained for the $\nu = 1/2$ state. The results seem to be reasonable and a further investigation shows that the found state has the property that the density is perfectly uniform throughout the system, see figure 4.4. A calculation shows that the mean density is $1/2$ up to the precision of at least 16 digits and the standard deviation of the single site density is as small as 10^{-12} for large systems. Even though the density is not as perfectly uniform as in figure 4.4 when we let the interaction range d be five or six the results are still strikingly uniform[14]. Another fact that leads us to believe that we have found a very special state is that the energy seems to be very low compared to other states[15]. Thus the obtained state has used the off diagonal elements of the Hamiltonian to reduce the energy in a very efficient way.

The results we obtained when we targeted $\nu = 1/3$ were quite discouraging compared to the $\nu = 1/2$ results. As shown in figure 4.5 the results are not looking good and we cannot observe any convergence. Furthermore the calculated $\nu = 1/3$ state does not have a uniform density distribution as shown in figure 4.6. As a matter of fact we were able to find another $\nu = 1/3$ state with considerably lower energy than the one found in figure 4.5 and, since the DMRG method obeys the variational principle, it is clear that we have not found the true ground state. This lower energy state is treated in figure 4.7 and it was surprisingly obtained by our algorithm when we kept only $m = 2$ states

[14] As an example, the standard deviation of the single site density is at the order of 10^{-7} for $d = 6$

[15] As we shall see soon it has even lower energy per site, and therefore also per particle, than ground states with lower densities ν.

in each iteration and it qualitatively has the structure hole-hole-particle-hole - hole-particle etc. The probable cause to the problems when we keep more states is that the DMRG method is not robust if the number of nonzero eigenvalues of the density matrix is smaller than the number of states m kept in each iteration.

Inspired by the results for the $\nu = 1/2$ state we investigate densities near $1/2$. As shown in figure 4.8 the state looks like the $\nu = 1/2$ state in the beginning and then it suddenly jumps. This is then repeated periodically. In order to gain further knowledge of what is going on we compute the expectation value of the density at different sites of a block of density $\nu = 0.499$. The results are shown in figure 4.9, 4.10 and 4.12. Furthermore, we present results with a targeted density $\nu = 0.501$ in figure 4.11.

We can clearly see that we recover the $\nu = 1/2$ state even though ΔH in (4.41) makes it energetically unfavourable to be in a state of that density. But when we continue the iterations something dramatic happens, as we were lead to believe by studying figure 4.8.

In order to analyze what is happening we recapitulate how we perform the calculations. In each iteration we add two sites at the center of the superblock which is the block which is used to find a target state $|\,\Psi\,\rangle$. This state is obtained by diagonalizing $H' = H + \Delta H = H + \gamma N^2(\hat{n} - \nu)^2$ and extracting the ground state $|\,\Psi\,\rangle$ of H'. What we find is that the $\nu = 1/2 \pm \varepsilon$ ground state is always the $\nu = 1/2$ state unless it is more favourable to place a hole or an extra particle at a localized position. No intermediate states are formed, i.e. in each iteration we add two sites to the superblock and we always find that we add zero, one or two particles to the system depending on the situation. An illustration of this is provided in figure 4.9 and figure 4.10 where we show the density distribution at the center of the superblock at two consecutive iterations. We observe a sudden transition and the net effect is that in the last iteration no particles were added to the superblock even though two more sites were added[16]. The exact shape of the hole or particle excitation happens to depend on the number of states m kept and the strength of the coupling γ but the number of holes or particles added is independent of these parameters. This is illustrated by the results displayed in figure 4.12, where we observe a more localized hole excitation. The results are also found to be practically independent of the range of interaction when $d = 4, 5$ and 6.

We can only speculate on how much our obtained $\nu = 1/2$ ground states has to do with known results for quantum Hall systems such as (4.16). It is possible that the restriction of the system to small circumferences L rules out these states but it is not certain. Hence, it would be very nice to be able to compare our DMRG results with the analytical ones corresponding to (4.15) and (4.16) in the cylinder geometry. However this is not manageable because we would be restricted to compare small systems with these results for practical reasons. Since we suffer from large edge-effects for these small systems this kind of comparison would not be meaningful.

[16] Adding more sites have the physical interpretation of increasing the magnetic flow perpendicular to the electron layer.

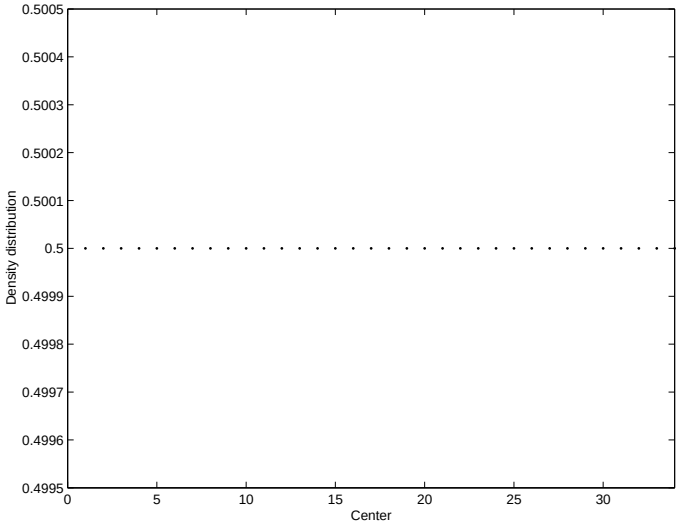

Figure 4.4: *A plot of the single site density* $\langle\, c_i^\dagger c_i \,\rangle$ *for a few sites close to the center of the superblock (at the right edge of the system). The calculations are from the same system and for the same number of states kept as in figure 4.3 and we have used* $d = 4$. *The distribution seems to be perfectly uniform and a calculation shows that the mean density is* $1/2$ *up to the precision of at least 16 digits. Furthermore the standard deviation of the single site density is as small as* 10^{-12}.

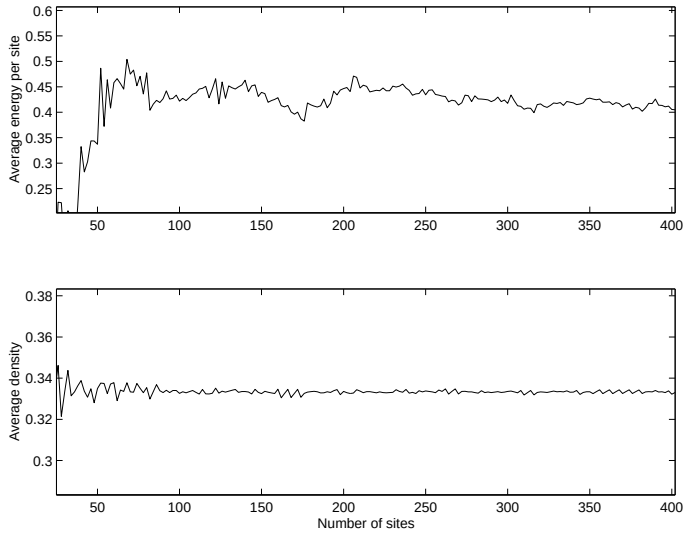

Figure 4.5: *Results from a DMRG calculation with the same conditions as in figure 4.3 except that the targeted density is* $\nu = 1/3$. *No smooth convergence is seen.*

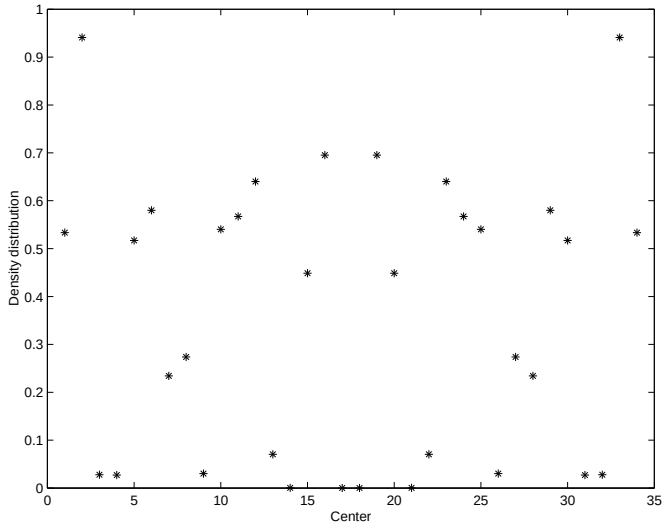

Figure 4.6: *The $\nu = 1/3$ density distribution close to the center of the block in the last iteration performed in figure 4.5.*

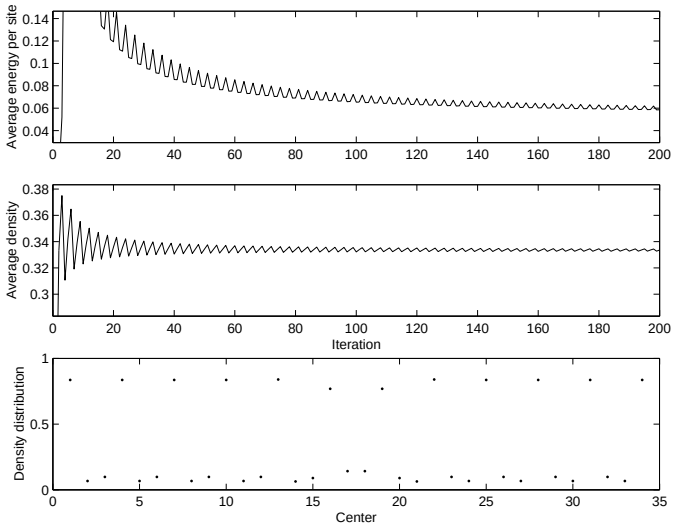

Figure 4.7: *An example of a state with considerably lower energy than the state in figure 4.5 even though the average density is approximately 1/3. Note that this state also has a non uniform density distribution.*

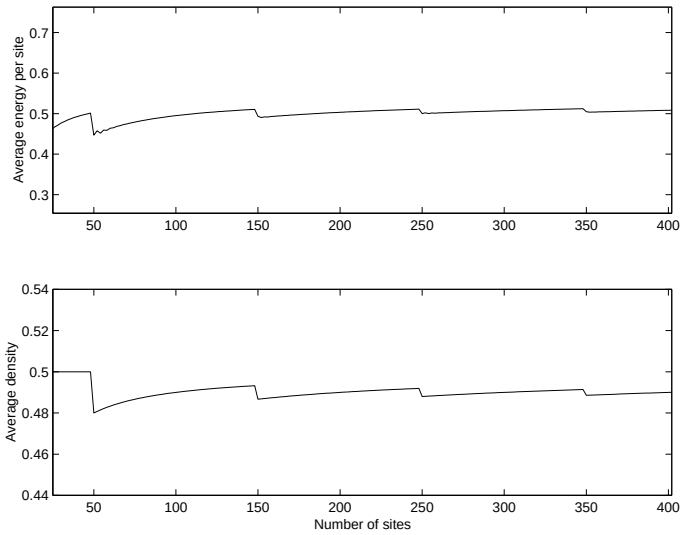

Figure 4.8: *Results from a DMRG calculation with the same conditions as in figure 4.3 except that the targeted density is* $\nu = 0.49$. *We observe a rather stable process with periodic jumps.*

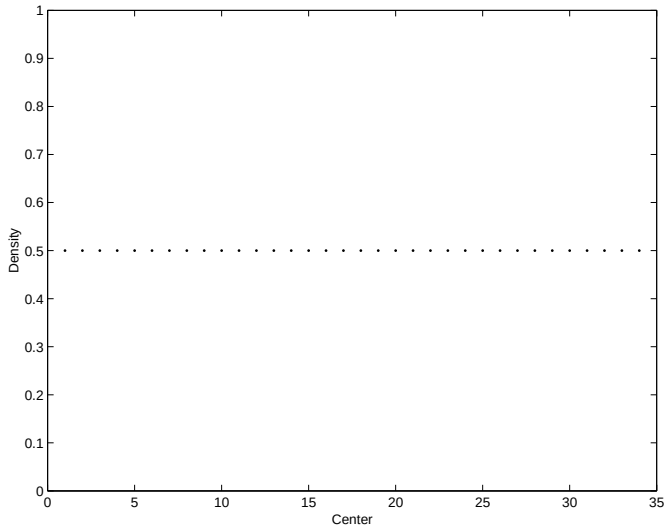

Figure 4.9: *This shows the expectation values of the single site density operators* $\langle\, c_i^\dagger c_i \,\rangle$. *This plot is identical to a plot of the densities in the* $\nu = 1/2$ *system although the results are obtained from the superblock configuration in a DMRG calculation with the targeted density* $\nu = 0.499$ *and 498 sites.*

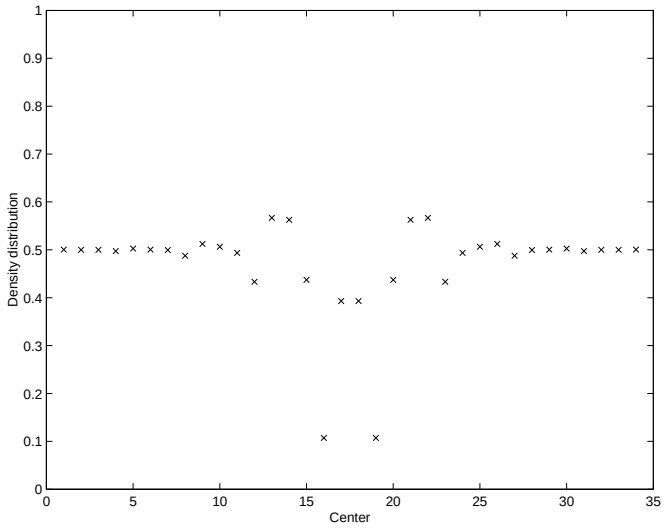

Figure 4.10: *This is the ground state obtained for the same system as in figure 4.9 when we performed one extra iteration. Hence the results are obtained from the superblock configuration in a DMRG calculation with the targeted density* $\nu = 0.499$ *and 500 sites. This plot indicates the possibility of a hole excitation in the* $\nu = 1/2$ *system. The results differ dramatically from those in figure 4.9 and it is obvious that something has happened in the last iteration. This localized object (or hole) has exactly the same number of particles as the* $\nu = 1/2$ *state with two sites less. I.e. the density jumps from a state with* $\nu = 1/2$ *to a state with* $\nu = 0.498$*. The center of the plot corresponds to the center of the superblock.*

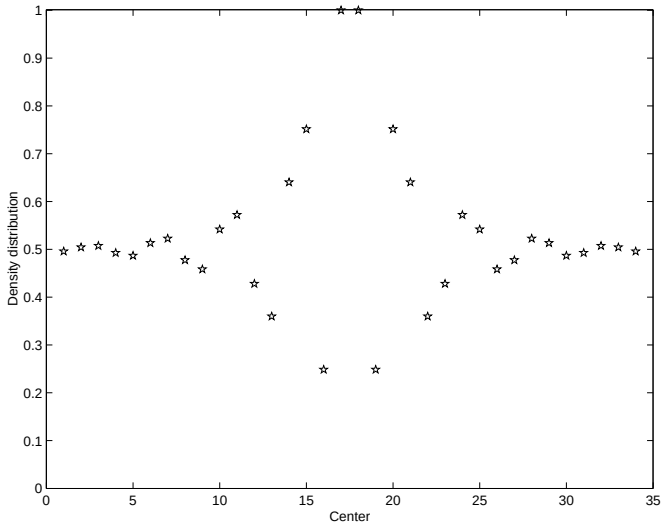

Figure 4.11: *Here we see evidence for a particle excitation. The results are obtained from a DMRG calculation with the targeted density* $\nu = 0.501$ *and 502 sites.*

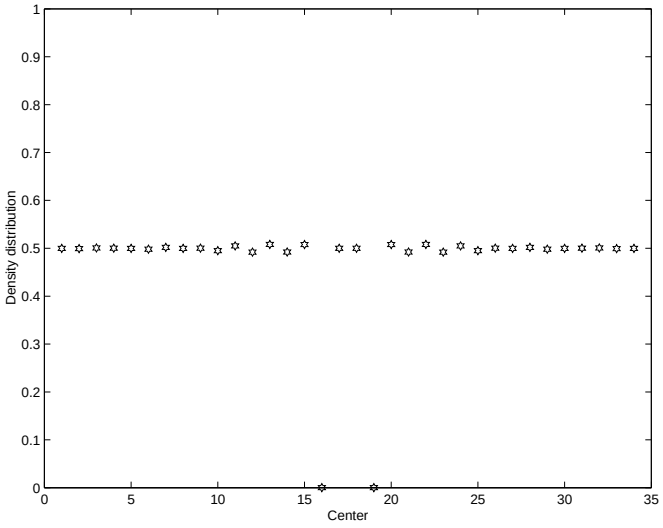

Figure 4.12: *A clear indication of holes. Note that two of the sites are practically empty* ($\langle c_i^\dagger c_i \rangle \approx 10^{-12}$)*. The typical length of the excitation is one magnetic length* ℓ*. The results are obtained by letting* $\gamma = 20$ *be much smaller than in the previous calculation shown in figure 4.10. The circumstances are equivalent of those in figure 4.10 in all other respects.*

Chapter 5

Conclusions and Outlook

In this thesis we have been able to reproduce some previously known results for one-dimensional nearest neighbor interacting systems using our own DMRG programs. These systems are the FM and AFM spin 1/2 Heisenberg, XY and Ising chains. The most striking results of the DMRG method, that we reproduced, are the highly nontrivial ground state results for the antiferromagnetic spin 1/2 Heisenberg chain.

Furthermore, we have mapped a two-dimensional quantum Hall system onto a one dimensional system and we have been able to handle interactions of longer range. We have also developed a method that makes it possible to study ground state properties at different densities, ν.

We looked for homogeneous QH states, since the Laughlin states have uniform density distribution, and found a very promising $\nu = 1/2$ state. Furthermore, we examined our $\nu = 1/2$ results and found some interesting properties such as very low energy, perfectly constant density distribution and localized particle as well as hole excitations. The excitations were observed when we targeted $\nu = 1/2 \pm \varepsilon$.

When we targeted other states than the $\nu = 1/2$ state we could not observe any smooth convergence and the states had nonuniform density distributions. However one observable effect was that the states had a symmetry in particles $\longleftrightarrow$ holes when $\nu \longleftrightarrow 1 - \nu$ for $\nu \leq 1/2$.

Despite our relative success, we have not been able to study the whole class of systems that we would like to have done. For practical reasons we were restricted to study the states on cylinders with relatively small circumferences L. Furthermore we were not able to compare our results with analytical ground state results because our systems are too large and the smaller systems that we studied suffer from disturbances from edge effects.

Our work has so far answered a few questions and raised many new. A natural way to continue this project would be to implement the finite DMRG method for a new, closely related, system. This new system is a system with periodic boundary conditions in both spatial directions, i.e. a torus. This would have a number of advantages. For example we would be able to treat smaller systems

with high accuracy. Therefore we would be able to compare our results with analytical results for this system [26, 27]. Moreover we would have no problems related to the edge effects and we would probably even be able to resolve the problem that forced us to study systems with small circumferences L. The only obvious problem with this approach is that the number of operators that we need to store grows with the size of the system. However this problem is not severe and a study of a closely related system, the quantum Hall effect in higher Landau levels, has in fact been performed by Shibata and Yoshioka [25].

As a matter of fact we have already dealt with many of the problems related to the finite size method when we have constructed our infinite method programs. The largest hurdle at the moment seems to be that we need to change programming language. It might also be cumbersome to find a matrix representation of the Hamiltonian since the single particle states on the torus are elliptical theta functions.

Bibliography

[1] S.R. White, Density Matrix Formulation for Quantum Renormalization Groups, Phys. Rev. Lett. 69, 2863 (1992).

[2] R.B. Laughlin, Anomalous Quantum Hall Effect: An Incompressible Quantum Fluid with Fractionally Charged Exitations, Phys. Rev. Lett. 50, 1395 (1983)

[3] K.G. Wilson, The renormailzation group: Critical Phenomena and the Kondo problem, Rev. Mod. Phys. 47, 773 (1975)

[4] S.R. White and R.M. Noack, Real-Space Quantum Renormalization Groups, Phys. Rev. Lett. 68, 3487 (1992).

[5] S.R. White, Density-matrix algorithms for quantum renormalization groups, Phys. Rev. B48, 10345 (1993).

[6] J.J. Sakurai, *Modern Quantum Mechanics* (Revised Edition) (Addison-Wesley Publishing company, New York, 1994)

[7] R.P. Feynman, *Statistical Mechanics: A set of lectures* (Benjamin, Reading, MA, 1972)

[8] F. Scheck, *Mechanics - From Newton's Laws to Deterministic Chaos*, (Springer-Verlag, Berlin Heidelberg New York, 1988)

[9] F. Gross, *Relativistic Quantum Mechanics and Field Theory*, (John Wiley & Sons Inc, New York, 1999)

[10] W. Heisenberg, Z. Phys. 38, 441 (1926)

[11] H. Bethe, Z. Phys. 71, 205 (1931)

[12] E. Ising, Z. Phys. 31, 253 (1925)

[13] D.C. Mattis, *The theory of Magnetism I: statistics and dynamics* (Springer-Verlag, Berlin Heidelberg New York, 1981)

[14] M. Karbach and G. Müller, Introduction to the Bethe ansatz I, cond-mat/9809162 (1998)

[15] L. Hultén, Ark. Met. Astron. Fysik 26A, Na. 11 (1938)

[16] B.T. Mattias, R. Bozorth and J. H. Van Vleck, Ferromagnetic Interaction in EuO, Phys. Rev. Lett. 7, 160 (1961)

[17] J. Cardy, *Scaling and Renormalization in Statistical Physics* (Cambridge University Press, Cambridge, 1996)

[18] L. Onsager, Phys Rev. 65, 117 (1944)

[19] S.M. Girvin, The Quantum Hall Effect: Novel exitations and Broken Symmetries, arXiv:cond-mat/9907002 (1999)

[20] L.D. Landau and E.M. Lifshitz, *Quantum Mechanics* (Pergamon Press, New York, 1994)

[21] S.A. Trugman and S. Kivelson, Exact results for the fractional quantum Hall effect with general interactions, Phys. Rev. B31, 5280 (1985)

[22] S.H. Simon, The Chern-Simons Fermi Liquid Description of Fractional Quantum Hall States, arXiv:cond -mat/9812186 (1998)

[23] E.H. Rezayi and N.Read, Fermi-liquid-like state in a half-filled Landau level, Phys. Rev. Lett. 72, 900 (1994)

[24] T. Xiang, Density-matrix renormailzation-group method in momentum space, Phys. Rev. B 53, R10445 (1996)

[25] N. Shibata and D. Yoshioka, Ground-State Phase Diagram of 2D Electrons in a High Landau Level: A Density-Matrix Renormalization Group Study, Phys. Rev. Lett. 86, 5755 (2001)

[26] F.M.D. Haldane, Fractional Quantization of the Hall Effect: A Hierarchy of Incompressible Quantum Fluid States, Phys. Rev. Lett. 51, 605 (1983)

[27] F.M.D. Haldane and E.H. Rezayi, Periodic Laughlin-Jastrow wave functions for the fractional quantized Hall effect, Phys. Rev. B 31, 2529 (1985)